

Physics of fluids & nonlinear physics

ARNAUD ANTKOWIAK¹
SORBONNE UNIVERSITÉ

December 7, 2025

¹arnaud.antkowiak@upmc.fr

Contents

Contents	3
1 Fluid Motion	7
1.1 Balance equation: variation, fluxes and production	7
1.1.1 Differentiation along motion	8
1.1.2 Volume variation of a material domain and integral derivation	8
1.1.3 Diffusive and convective fluxes	10
1.1.4 Advection	10
1.1.5 Diffusion	11
1.1.6 Conservation of a quantity. Application to mass conservation	11
1.1.7 Conservation of a diffusing passive scalar. Convection-diffusion equation .	12
1.2 Forces	13
1.2.1 Pressure	13
1.2.2 Stresses	14
1.2.3 Body forces	15
1.3 Fluid equilibrium	15
1.4 Fluid motion	17
1.4.1 Equation for momentum conservation	17
1.4.2 Energy conservation	17
1.5 Constitutive laws	19
1.6 Wrapping up: The Navier-Stokes and energy equations	20
1.6.1 The Navier-Stokes equation	20
1.6.2 The energy equation	21
2 Boundary conditions and interfaces	23
2.1 Fluxes at boundaries: impermeability and imbibition	23
2.2 Phenomenological conditions: adherence and continuity	27
2.3 Where is the interface?	28
2.3.1 Kinematic boundary condition.	28
2.3.2 Surface geometry I. Normals.	29
2.4 Capillarity	29
2.4.1 Cohesion	31
2.4.2 Surface tension	31
2.4.3 Surface geometry II. Curvature.	31
2.5 Young-Laplace's pressure jump	33
2.5.1 Surface tension?	35
2.5.2 Stress (dis-)continuity	36
2.6 Equilibrium shape for a meniscus	36

3 Viscous flows	39
3.1 Low-Re number flows	39
3.2 Stokes flow's properties	41
3.3 Moving in a viscous world	42
3.3.1 Point force induced flow: the Stokeslet	43
3.3.2 The motion of slender objects	44
4 Thin viscous films	47
4.1 A rippled paint coat	47
4.2 Power & limits of dimensional analysis	47
4.3 Quick physical analysis and order of magnitude estimate	48
4.4 Detailed asymptotic analysis: thin film flow	49
4.4.1 Preliminary: mass conservation	50
4.4.2 Stress condition at the interface	50
4.4.3 Flow motion: analysis of the momentum equation	51
4.4.4 Structure of the flow within the film	52
4.4.5 Connecting the free surface deformation with the flow	53
4.4.6 Thin film equation	53
4.5 Epilogue: relaxation time for a rippled liquid film	54
5 Planetary flows and the effect of rotation	55
5.1 Rotating fluids	55
5.2 Fluid flows on a rotating sphere	56
5.2.1 Governing equations in spherical coordinates	56
5.2.2 A local cartesian coordinate system	57
5.2.3 Scaling the equations	57
5.2.4 Nondimensionalisation: a worked-out example	58
5.2.5 A hierarchy of models for planetary flows	59
5.3 Geostrophic equilibrium	60
5.4 Application: wind over France	60
5.5 Oceanic and atmospheric circulation	61
5.5.1 Oceanic circulation: wind-induced gyres	61
Bibliography	65
Index	68

Modelling fluids

▷ **The birth and death of a bubble.** Take a simple bubble grown and swollen by carbon dioxide diffusion in a fizzy drink. When the bubble detaches from its nucleation point, it first starts by vibrating. This is the characteristic noise of bubbling beverages, and it is actually rooted in a competition between bubble compressibility and liquid inertia (Minnaert, 1933). After these first few instants (lasting a few milliseconds) where inertia and compressibility matter, the bubble is taken upwards as a result of its buoyancy. During this stage, a complex wake develops behind the bubble where vortices entangle, leading to a nice zigzag and then spiralling ascending motion (Mougin & Magnaudet, 2001). In this phase lasting few tenths of a second, the bubble motion is no more influenced by compressibility but now by gravity, fluid inertia and viscosity. The bubble now reaches the top of the glass, and squeezes a thin liquid film that will ultimately form the bubble cap. This bubble cap then slowly drains under the sole influence of gravity and capillarity for times that can extend to several tens of a second, depending on the nature of the liquid. At some point, the cap will be so thin that van der Waals effects will kick in and promote a destabilisation of the liquid film in a few microseconds. The punctured film will then be unbalanced and pulled away. In this opening regime of a few milliseconds duration, the dominating effects are now the liquid film inertia and the pulling action of capillarity. At this point, what is left of the bubble is really a hole of the liquid surface. Interestingly, rather than to be simply filled in, the interface will shed capillary ripples trains that will quickly converge to the cavity bottom (Ghabache *et al.*, 2014). These waves result from a balance between liquid inertia and capillarity. The cavity will then start to violently collapse in a singular event where pressure and velocity will tend to diverge. What happens near the singularity is still a matter of debate today. Right after the collapse we observe a cavity reversal and a thin liquid jet forms, and breaks under the combined action of jet inertia and capillarity. The newly formed droplets will then oscillate and possibly evaporate during their free flight.

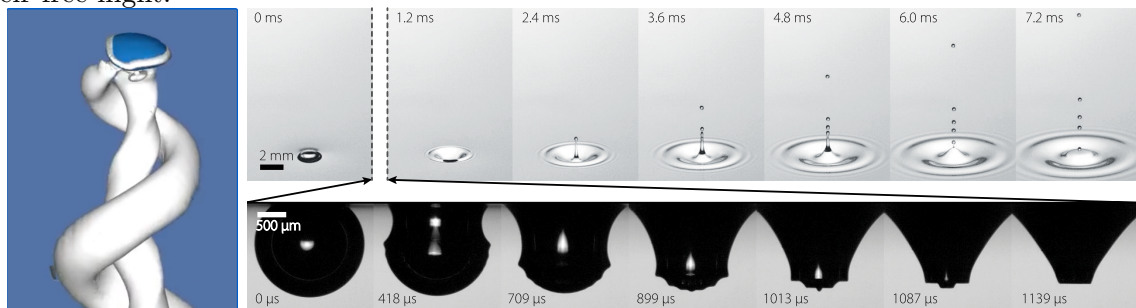


Figure 1: Left: ascending bubble influenced by its spiralling vortex wake (taken from [Basilisk](#)'s website). Right: rapid sequence of events following the bursting of the bubble (Ghabache *et al.*, 2014).

In this example taken from everyday life, we see that fluid motions, even for a single setup, can be influenced by various effects (phase change, acoustic waves, capillary instability, electrostatic interactions...) that over a wide variety of length- and timescales. Most importantly we see that the dominant effects change over time and space.

In this lecture we aim to give clues for describing such problems, making use of a palette of approaches, starting with dimensional analysis, quick order of magnitudes estimates or more refined asymptotic analyses.

Chapter 1

Fluid motion

The governing equations for fluid motion express truly simple physical principles, namely:

- **mass** conservation (the mass $m(t)$ of a fluid particle is constant),
- **momentum** conservation (a fluid particle's momentum obeys Newton's second law $m\boldsymbol{\gamma} = \Sigma\boldsymbol{F}$), and
- **energy** conservation (the energy of a fluid particle follows the first principle of thermodynamics).

In this introduction we will review the derivation of the fluid mechanics equations by expressing these fundamental conservation principles. It will be seen in particular that the derivation of the equations follows invariably the following scheme:

1. Identify the conservation law for the quantity under interest,
2. Establish a balance equation for the quantity over a finite volume of fluid,
3. Write the limiting form of this balance at the local (*fluid particle*) level,
4. Make use of constitutive laws to obtain a final, closed-form, version of the equation.

In this chapter we will obtain the mass and momentum conservation equations governing the flowing of fluids.

1.1 Balance equation for an integrated quantity: variation, fluxes and production

To start with, let's write the most general form of the balance of a quantity c integrated over a given volume V :

$$\underbrace{\frac{d}{dt} \iiint_V c dV}_{\text{Variation}} = - \underbrace{\iint_{\partial V} \boldsymbol{j} \cdot \boldsymbol{n} dS}_{\text{Exchange}} + \underbrace{\iiint_V \varphi dV}_{\text{Production}}. \quad (1.1)$$

This equation expresses that the *variation* of an integrated quantity c in V is given by a balance of entering/leaving quantity into/from the domain (*exchange*) and the possible *production* (or destruction) of c inside V^1 . While the production term is without ambiguity, several comments are called for the other terms appearing in this balance. First, the exchange term characterises exchanges across surfaces bounding the fluid volume. This term involves **fluxes**, measuring the quantity under interest crossing the boundaries per unit surface and time. Fluxes will be examined momentarily in §1.1.3.

The left hand side of the equation characterises the variation of the quantity with the help of the derivative of an integral, and the precise meaning of this notation has to be clarified before going further. If the considered volume is fixed, the derivation process is easy as we can just

¹This relation is obtained on **physical** grounds.

swap derivation and integration. But if the domain is moving or deforming, care must be taken in writing this derivation. In the following we analyse how to write the variation of a quantity attached to a fluid particle, or integrated over a given fluid volume.

1.1.1 Differentiation along motion

One technical issue with the simple conservation laws mentioned at the beginning of the chapter is that they are expressed at the fluid particle level (e.g. the mass of a fluid particle is preserved, the momentum of a fluid particle is conserved or affected by surrounding forces). This seems quite natural, but it conflicts with our usual representation of space. Let's clarify what we mean by this by considering a typical fluid flow, for example the one around an airplane wing. Typically we are interested in estimating the forces exerted by the flowing fluid on a the plane, and this requires to build a knowledge of the stresses exerted on the wing. The pressure applied at one given point of the wing is ultimately a consequence of conservation laws, but we clearly do not want to track the life and trajectory of every fluid particle² that will ever very shortly pass in the neighbourhood of the airplane to get this prediction! Rather we seek to make sure that the conservation laws are satisfied while looking at a fixed point of space (and therefore see quite a number of fluid particles passing there). In order to express the conservation laws governing the motion, we thus need to describe the variation of any quantity attached to a fluid particle, such as a concentration or its momentum.

Let's take the example of a concentration field $c(\mathbf{x}, t)$. Following a fluid particle in its motion, we can write down how the concentration attached to it varies with time:

$$c(\mathbf{x} + \mathbf{u} \delta t, t + \delta t) - c(\mathbf{x}, t) = \delta t \underbrace{\left(\frac{\partial c}{\partial t} + (\mathbf{u} \cdot \nabla) c \right)}_{\frac{dc}{dt}} + \mathcal{O}(\delta t^2), \quad (1.2)$$

where we made the rate of concentration change $\frac{dc}{dt}$ appear. Note that this quantity differs from $\frac{\partial c}{\partial t}$ which would rather measure the variation of c at a fixed (*eulerian*) position of space, without following the fluid particle. The operator $\frac{d}{dt}$ is called **particle derivative** (or material, or convective, or Lagrangian derivative):

$$\frac{dc}{dt} \equiv \frac{\partial c}{\partial t} + (\mathbf{u} \cdot \nabla) c. \quad (1.3)$$

As an illustration, the equation governing the concentration field transported by a flowing fluid without considering diffusion effects is therefore simply:

$$\frac{dc}{dt} = 0 \quad \text{or} \quad \frac{\partial c}{\partial t} + (\mathbf{u} \cdot \nabla) c = 0. \quad (1.4)$$

We note also that the *acceleration* of a fluid particle is simply $\frac{d\mathbf{u}}{dt}$.

1.1.2 Volume variation of a material domain and integral derivation

We will now give a meaning to the derivation of an integral performed over a deformable domain. To start with, let's consider the quite specific (but still really common) case of a **material** domain, i.e. we follow the same fluid particles though time. As time flows this domain may see its volume change as indicated on figure 1.1, hence as:

$$\frac{d}{dt} \iiint_V dV = \oint_{\partial V} \mathbf{u} \cdot \mathbf{n} dS \quad \left(= \iiint_V \nabla \cdot \mathbf{u} dV \right). \quad (1.5)$$

²There is actually an alternate form of the fluid mechanics equations called *Lagrangian fluid mechanics* that exploit this viewpoint, but it gets quickly untractable and only a few specific flows can be described with this approach (Bennett, 2006).

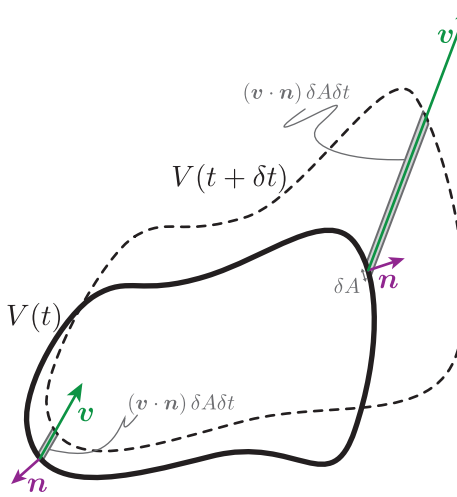


Figure 1.1: A material volume is transported by a velocity field \mathbf{u} . Each portion δA of the domain boundaries is advected with \mathbf{u} and this yields a volume change $(\mathbf{u} \cdot \mathbf{n}) \delta A \delta t$ during δt . The resulting total volume change rate $\frac{dV}{dt}$ is given by $\iint (\mathbf{u} \cdot \mathbf{n}) dA$.

▷ **Signification of the divergence.** The previous relation allows to shed light on the divergence of a velocity field \mathbf{u} . Actually, consider a material volume $\tau(t)$ constituted with the same fluid particles. The previous balance might be rewritten with the help of the divergence theorem as:

$$\frac{d\tau}{dt} = \iint \mathbf{u} \cdot \mathbf{n} dS \quad (1.6)$$

$$= \iiint \nabla \cdot \mathbf{u} dV. \quad (1.7)$$

Thus in the limit where $\tau(t)$ is really small (in fact sufficiently small so that we can consider $\nabla \cdot \mathbf{u}$ constant throughout the domain), we can write:

$$\lim_{\tau \rightarrow 0} \frac{1}{\tau} \frac{d\tau}{dt} = \nabla \cdot \mathbf{u}. \quad (1.8)$$

The divergence of a velocity field can therefore be understood as the *rate of volume change of a fluid particle*.

▷ **Integral derivation.** We now have the toolset enabling the clarification of the derivation of the integral over a material domain $V(t)$. Let's focus on the variation of the following quantity:

$$\frac{d}{dt} \iiint_{V(t)} \theta dV.$$

To shed some light over this quantity, let's divide mentally the domain in a multitude of tiny cubes or fluid particles. As the fluid domain moves, the value of θ will change for all fluid particles at the rate $\frac{d\theta}{dt}$. Moreover the integration element dV will change as well with the rate

$(\nabla \cdot \mathbf{u}) dV$. In other words^{3,4} :

$$\frac{d}{dt} \iiint_{V(t)} \theta dV = \iiint_{V(t)} \frac{d\theta}{dt} dV + \iiint_{V(t)} \theta \underbrace{\frac{d(dV)}{(\nabla \cdot \mathbf{u}) dV}}_{(\nabla \cdot \mathbf{u}) dV} \quad (1.9)$$

Having clarified the meaning of the derivation of an integrated quantity, we now turn to examine the exchange term in (1.1) involving fluxes.

1.1.3 Diffusive and convective fluxes

When flowing, fluids transport mass, but also chemical species, energy and momentum. To describe the corresponding transport modes, we will use the notion of **flux** (of mass, momentum, energy). The vectorial flux \mathbf{j} characterises the transfer of a quantity across an oriented surface $\delta A \mathbf{n}$ per unit time:

$$\mathbf{j} \cdot \mathbf{n} \delta A \quad (1.10)$$

1.1.4 Advection

The first transport mode for mass, momentum or energy is advection. Let's suppose that a given field, for example concentration c again, is **transported** with the fluid at velocity⁵ \mathbf{u} , i.e. each fluid particle conserves its concentration. Consider now the **fixed** surface element δA represented figure 1.2. The matter quantity c flowing across the surface⁶ during a short moment δt is $(c \mathbf{u} \cdot \mathbf{n}) \delta A \delta t$. As a result the matter quantity transported across δA per unit surface and per unit time is $\mathbf{j}_{\text{adv}} \cdot \mathbf{n}$ where

$$\mathbf{j}_{\text{adv}} = c \mathbf{u} \quad (1.11)$$

is the matter **flux** associated with advection. Now if the surface element is **mobile** and moves

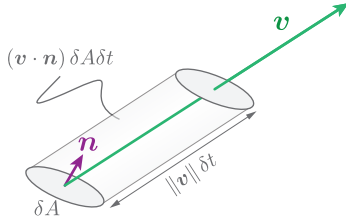


Figure 1.2: A surface portion δA of normal \mathbf{n} is traversed by a fluid volume $(\mathbf{u} \cdot \mathbf{n}) \delta A \delta t$ during δt . This volume is counted positively if \mathbf{u} points towards the same half-space as \mathbf{n} (in which case $\mathbf{u} \cdot \mathbf{n} > 0$), and negatively otherwise.

at velocity \mathbf{w} , the advection flux generalises to:

$$\mathbf{j}_{\text{adv}} = c (\mathbf{u} - \mathbf{w}) \quad (1.12)$$

We note that in the context of a **material domain**, i.e. moving with the same velocity as the fluid, we get $\mathbf{w} = \mathbf{u}$ and the advection flux cancels out by construction.

³This relation is obtained on **mathematical** grounds.

⁴We note that this relation can directly be generalised to the case where the domain moves with a velocity differing from that of the fluid (fictitious velocity, flame propagation, balance over a domain moving with a wave). In this case, it suffices to replace \mathbf{u} with the domain velocity \mathbf{w} .

⁵The velocity \mathbf{u} is understood as the average velocity of molecules in the vicinity of the considered point. With this definition we see that the velocity already incorporates diffusion effects. In mixtures chemical species usually have different velocities that need a careful treatment (Bird *et al.*, 2002, §17.7).

⁶We here make use of the fact that a slanted cylinder of length $\|\mathbf{u}\| dt$ is the same as a right cylinder of same height $(\mathbf{u} \cdot \mathbf{n}) dt$. This is Cavalieri's principle – which can also be demonstrated with a simple integration.

1.1.5 Diffusion

Now, even without any underlying net flow, simple matter (species concentration), energy or momentum inhomogeneities will give rise to transfer spontaneously. This phenomenon is a manifestation of random molecular motions which yield effective macroscopic exchanges (Leal, 2007). These **diffusive** exchanges are quantified per unit surface and time with the **diffusive flux** \mathbf{j}_{diff} . Even if a detailed modelling of these exchanges is a complex feat, they can nonetheless be described with phenomenological relations (constrained with thermodynamical arguments) such as Fick's law for mass transport for example (see §1.5).

1.1.6 Conservation of a quantity. Application to mass conservation

Now that the derivation of an integral has been elucidated, we are in a position to use equation (1.1) which expresses the general conservation of a quantity, for either a fixed or moving domain. Choosing one type of domain or another is largely a matter of context. For example we may consider a moving domain to establish the momentum conservation equation of a given fluid portion. A balance over a fixed domain may also present some interest, when designing for example the evolution of a quantity traversing a fixed mesh cell in a numerical code. Depending on the application, we will choose the more relevant viewpoint.

In order to clarify the use of balances over fixed or moving domains, let's now establish the mass conservation equation (without production nor destruction of mass), first in a fixed domain and then in a moving one.

1. **Mass conservation in a fixed domain V_{fixed} .** The balance equation (1.1) reads :

$$\frac{d}{dt} \iiint_{V_{\text{fixed}}} \rho dV = - \oint_{\partial V_{\text{fixed}}} \rho \mathbf{u} \cdot \mathbf{n} dS. \quad (1.13)$$

The domain being fixed, we let the derivation enter in the integral:

$$\iiint_{V_{\text{fixed}}} \frac{\partial \rho}{\partial t} dV = - \oint_{\partial V_{\text{fixed}}} \rho \mathbf{u} \cdot \mathbf{n} dS, \quad (1.14)$$

and, on applying the divergence theorem, we obtain:

$$\iiint_{V_{\text{fixed}}} \frac{\partial \rho}{\partial t} + \nabla \cdot (\rho \mathbf{u}) dV = 0. \quad (1.15)$$

Further noting that this balance is actually true for every possible domain, it follows that the integrand actually vanishes:

$$\frac{\partial \rho}{\partial t} + \nabla \cdot (\rho \mathbf{u}) = 0. \quad (1.16)$$

This is the **continuity equation**⁷ that embodies mass conservation. This type of reasoning exploiting the validity of an integral expression for any volume to obtain a relation at the fluid particle (or *local*) level is very common.

2. **Mass conservation for a material domain $V(t)$.** This time there is no flux term because no fluid particle enters nor leaves the material domain, by definition. The balance equation (1.1) then reads:

$$\frac{d}{dt} \underbrace{\iiint_{V(t)} \rho dV}_{m(t)} = 0. \quad (1.17)$$

⁷This denomination has been used for a long time, but is actually not really justifiable...

But as the domain is now moving, we have to apply the integral derivation procedure seen earlier:

$$\frac{d}{dt} \iiint_{V(t)} \rho dV = \iiint_{V(t)} \frac{d\rho}{dt} + \rho \nabla \cdot \mathbf{u} dV = 0. \quad (1.18)$$

From the latter we recover again the continuity equation (1.16).

▷ **Conservation of a quantity per unit mass.** Thanks to the continuity relation it is possible to obtain a simplified expression for the transport of a quantity per unit mass ξ (i.e. such that the quantity associated with a fluid particle be $\rho\xi$):

$$\frac{d}{dt} \iiint_{V(t)} \rho\xi dV = \iiint_{V(t)} \rho \frac{d\xi}{dt} dV. \quad (1.19)$$

We let the reader demonstrate this relation.

▷ **The incompressible fluid.** A recurring case of great practical value is that of an **incompressible evolution** where we do *not* suppose that the whole fluid a constant density, but rather that each fluid particle conserves its density. This implies:

$$\frac{d\rho}{dt} = 0 \quad \text{and therefore} \quad \nabla \cdot \mathbf{u} = 0. \quad (1.20)$$

A velocity field \mathbf{u} satisfying the zero divergence property qualifies as a *solenoidal* field.

1.1.7 Conservation of a diffusing passive scalar. Convection-diffusion equation

Let's consider again a concentration field c advected in a fluid domain with the velocity field \mathbf{u} . Due to molecular thermal agitation, this field is also subject to diffusion phenomena characterised by the flux \mathbf{j}_{diff} . Here again we can obtain the evolution equation for the concentration by following two different routes:

1. By considering a **fixed domain** V_{fixed} . In this case, and in absence of any source/sink for the concentration, we will simply write that the total variation is given by the sum of the fluxes:

$$\frac{d}{dt} \iiint_{V_{\text{fixed}}} c dV = - \oint_{\partial V_{\text{fixed}}} (\mathbf{j}_{\text{conv}} + \mathbf{j}_{\text{diff}}) \cdot \mathbf{n} dS,$$

so that:

$$\iiint_{V_{\text{fixed}}} \frac{\partial c}{\partial t} dV = - \iiint_{V_{\text{fixed}}} \nabla \cdot (\mathbf{j}_{\text{conv}} + \mathbf{j}_{\text{diff}}) dS.$$

Anticipating on §1.5 by writing the diffusive flux with Fick's law $\mathbf{j}_{\text{diff}} = -D\nabla c$ we obtain at the local level:

$$\frac{\partial c}{\partial t} + \nabla \cdot (c\mathbf{u}) = \nabla \cdot (D\nabla c) \quad (1.21)$$

For an incompressible evolution with a constant diffusion coefficient, this equation reduces to the classic **advection-diffusion equation**:

$$\frac{\partial c}{\partial t} + (\mathbf{u} \cdot \nabla) c = D\nabla^2 c. \quad (1.22)$$

2. Or by considering a **material domain** V_{mat} . This time there is no convective flux by construction (see §1.1.4) but only a diffusive flux:

$$\frac{d}{dt} \iiint_{V_{\text{mat}}} c dV = - \oint_{\partial V_{\text{mat}}} \mathbf{j}_{\text{diff}} \cdot \mathbf{n} dS,$$

so that, by deriving the integral over the material domain:

$$\iiint_{V_{\text{mat}}} \frac{dc}{dt} + c(\nabla \cdot \mathbf{u}) dV = \iiint_{V_{\text{mat}}} \nabla \cdot (D \nabla c) dS.$$

This relation holds true for every possible domain, and as a result we retrieve the local form of equation (1.21).

1.2 Forces

Before moving on to the writing of the momentum equation, it is necessary to reflect on the forces exerted on fluid particles, that differ from forces exerted on isolated bodies. As other continuum media, fluids carry force fields that determine their equilibrium (when the net force contribution is zero) or their motion. If each fluid particle is subject to *body forces*, it is also exposed to *surface forces* called **stresses**, as for example pressure (Fig. 1.3) that we now examine.

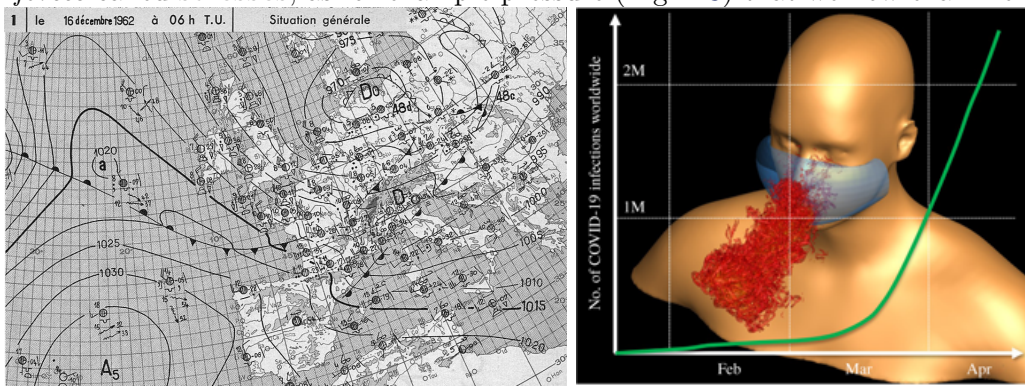


Figure 1.3: **Illustrations of pressure forces in daily-life phenomena.** Left: France isobaric map from December, 16 1962. The map reveals low-pressure area and anticyclones (high-pressure area). The clustering isobars near Corsica are a signature of the violent winds that swept the region (force 12 on the Beaufort scale i.e. the threshold for hurricanes for sailors ; 216 km/h at the cap Corse). Source: <http://tempetes.meteo.fr>. Right: a coughing event is associated with a violent lung compression. The resulting overpressure drives a rapid airflow that may torn and transport liquid droplets and aerosols (Mittal *et al.*, 2020).

1.2.1 Pressure

▷ **Archimedes principle without equation.** Consider a fluid at equilibrium in the gravity field (Fig. 1.5). Let's isolate now mentally a fluid portion. It experiences from the gravity field a force corresponding to its *weight* \mathbf{P} pointing downwards. It also bears *pressure forces* from the surrounding fluid. Since the fluid portion is at equilibrium, the net pressure force has to balance the weight (equal in intensity but opposite in direction). Now if in our mind experiment we were to replace the fluid portion by a solid object, the resulting action of the external forces would not change: the net force exerted by pressure forces is still equal in intensity to the weight of the fluid “displaced” by the solid. The resultant of pressure forces corresponds to the *buoyancy* (Lighthill, 1986). Of course if the solid is denser (or less dense) than the surrounding fluid, the equilibrium would be lost and fluid/body motion would set in.

Pressure is a force per unit surface which is **normal** to the considered surface⁸. This type of distributed force in a fluid is a specificity of continuum media, and is referred to as **stress**. Here

⁸We may see this feature as the *definition* of a fluid, i.e. a medium unable to resist shear (Prandtl & Tietjens, 1957; Batchelor, 1967, §1.3). A shear stress would therefore unvariably set the fluid into motion.

the corresponding stress expression is therefore:

$$d\mathbf{f} = -p \mathbf{n} dS. \quad (1.23)$$

The minus sign translates the state of compression in which fluids generally are (so that pressure is a positive quantity, unless in very specific cases of tensile solicitations of fluids).

► **Pressure as a body force.** On figure 1.4 we illustrate the action of pressure forces exerted on a small cylindrical fluid portion. The portion has a base S and a height dn leaning on two isobars p and $p+dp$. The action of pressure forces on the side of the cylinder is zero by symmetry, so that the net pressure force is simply the sum of the contributions exerted on each bounding face : $S p$ and $-S (p + dp)$ (let's count positively – and arbitrarily – the forces oriented along the pressure gradient), which is $-S dp$. If we divide this force by the volume of the small element, $S dn$, it appears that pressure forces can be perceived as a body force of intensity $-\frac{\partial p}{\partial n}$ acting along ∇p . In other words pressure forces may be understood as body forces of intensity $-\nabla p$; this is the meaning of this term appearing in both Euler and the Navier–Stokes equations. This

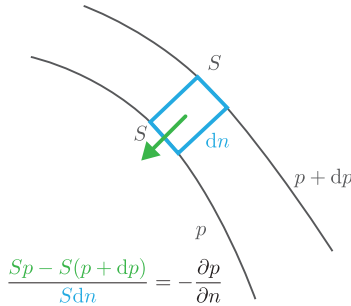


Figure 1.4: Writing down a force balance on a volume portion $S dn$ leaning on two isobars (of level p and $p + dp$), we see that the pressure action may be understood as a body force per unit volume of intensity $-\frac{\partial p}{\partial n}$.

is here a physical interpretation of the divergence theorem which would have given directly:

$$-\iint_{\partial V} p \mathbf{n} dS = -\iiint_V \nabla p dV.$$

1.2.2 Stresses

In the general context of a flowing fluid, stress has no particular reason to be aligned with the normal – and, as a matter of fact, it is not. But multiplying the normal vector \mathbf{n} with a scalar can only give another vector still aligned with \mathbf{n} , and using the cross product is of no help either because the cross product between any vector and \mathbf{n} can only give a vector perpendicular to \mathbf{n} . So we need another mean to obtain a vector arbitrarily oriented from the unique knowledge of \mathbf{n} . The mathematical object allowing to perform this operation is the 2-rank tensor. On using Einstein notations, this gives:

$$df_i = \sigma_{ij} n_j dS. \quad (1.24)$$

We have here to remember that this object is only a mean to obtain $d\mathbf{f}$ not necessarily aligned with \mathbf{n} .

Of course it is possible to obtain the simple case of a stress aligned with \mathbf{n} using this formalism. As an example, the stress tensor of a fluid at rest (eq. 1.23) is:

$$\sigma_{ij} = -p \delta_{ij}. \quad (1.25)$$

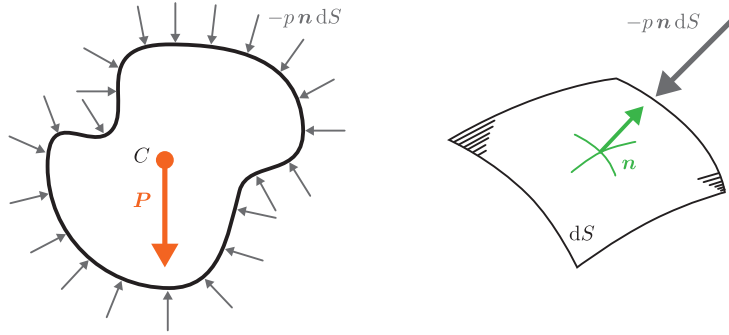


Figure 1.5: Left: when at equilibrium in the gravity field, every fluid portion experiences pressure forces that exactly balance the weight action \mathbf{P} . Right: the pressure stress is normal to each surface element.

It is possible to show that this stress tensor $\boldsymbol{\sigma}$ is necessarily a symmetric tensor, i.e. $\sigma_{ij} = \sigma_{ji}$ (Batchelor, 1967, §1.3). The demonstration's main idea is to write an angular momentum balance at the fluid particle level; the only dominant term in this equation involves the antisymmetric part of $\boldsymbol{\sigma}$. As it is not balanced by any term, it necessarily vanishes. There is one exception however: in the very particular case of a *moment density*, as in active matter or certain magnetic colloids, this term can be balanced and the tensor be non-symmetric (see for example the study of Soni *et al.*, 2019).

1.2.3 Body forces

Fluids are also subject to more conventional body forces, which can be magnetic, electrostatic, gravity or result from non-inertial effects (think of centrifuge or Coriolis pseudo-forces). On noting \mathbf{f} the body force **per unit mass** acting on the fluid particle level, we can write the net body force exerted on a fluid portion V as:

$$\iiint_V \rho \mathbf{f} dV. \quad (1.26)$$

▷ **To summarize.** The net force acting on a fluid portion V is the sum of surface and body forces:

$$\oint\!\oint_{\partial V} \boldsymbol{\sigma} \cdot \mathbf{n} dS + \iiint_V \rho \mathbf{f} dV. \quad (1.27)$$

1.3 Fluid equilibrium

At equilibrium, pressure and body force exerted on any part V of a fluid balance each other:

$$\iiint_V \rho \mathbf{f} dV - \iint_{\partial V} p \mathbf{n} dS = 0,$$

or, on using the divergence theorem:

$$\iiint_V (\rho \mathbf{f} - \nabla p) dV = 0. \quad (1.28)$$

This relation being verified for *any* fluid domain, we necessarily get at the local level:

$$\rho \mathbf{f} = \nabla p. \quad (1.29)$$

And we recover here the pressure force expressed as a body force $-\nabla p$.

Remark: Only those density and force fields such that $\rho \mathbf{f}$ can be expressed as a gradient allow to reach hydrostatic equilibrium (counter-example: the baroclinic instability developing when iso- p differ from iso- ρ , or in other words as soons as pressure is not a simple function of ρ).

▷ **The case of conservative forces.** Conservative forces derive from the potential Ψ :

$$\mathbf{f} = -\nabla\Psi, \quad (1.30)$$

so that

$$-\rho\nabla\Psi = \nabla p, \quad (1.31)$$

and therefore

$$\nabla\rho \times \nabla\Psi = 0. \quad (1.32)$$

The iso- ρ (isopycnals) are then superimposed to equipotentials, themselfed superimposed with isobars.

Consequence: in such a system, a free surface corresponding to $p = 0$ for example will also be an equipotential $\Psi = \text{const.}$

▷ **Example: the equilibrium of a rotating fluid.** Let's consider a rotating container filled with liquid. The container rotates at angular velocity Ω in the gravity field (the axis of rotation is vertical, i.e. directed along \mathbf{e}_z). In the rotating frame, each fluid particle experiences gravity but also the centrifuge pseudo-force:

$$\rho\mathbf{f}_{\text{cent}} = -\rho\boldsymbol{\Omega} \times (\boldsymbol{\Omega} \times \mathbf{r}). \quad (1.33)$$

Here $\boldsymbol{\Omega} = \Omega \mathbf{e}_z$. We can then write:

$$\rho\mathbf{f}_{\text{cent}} = \rho\Omega^2 r \mathbf{e}_r = -\rho\nabla\Psi_{\text{cent}}, \quad (1.34)$$

where

$$\Psi_{\text{cent}} = -\frac{1}{2}\Omega^2 r^2 = -\frac{1}{2}\Omega^2 (x^2 + y^2). \quad (1.35)$$

Adding gravity effects with $\Psi_{\text{grav}} = gz$ we get

$$\Psi_{\text{tot}} = \Psi_{\text{grav}} + \Psi_{\text{cent}} = gz - \frac{1}{2}\Omega^2 (x^2 + y^2). \quad (1.36)$$

We here remark that the equipotentials are paraboloids. As a result the free surface characterised with $p = 0$ ⁹ will also adopt a paraboloidal shape:

$$z_{\text{surf}} = \frac{1}{2} \frac{\Omega^2}{g} r^2 + \text{const.} \quad (1.37)$$

▷ **Exercise: fluid planet equilibrium.** Consider a self-gravitating fluid sphere. The gravity force per unit mass \mathbf{f} exerted on each fluid particle derives from the gravity potential Ψ such that:

$$\nabla^2\Psi = 4\pi G\rho, \quad (1.38)$$

⁹see chapter 2 for a discussion of the hypotheses behind this boundary condition.

where \mathcal{G} is the universal gravitational constant. With the help of the hydrostatic equation, and supposing that the fluid has a constant density¹⁰ ρ_0 , show that the radial pressure profile satisfies:

$$p(r) = \frac{2}{3}\pi\mathcal{G}\rho_0^2(R^2 - r^2), \quad (1.39)$$

with R the planet radius.

1.4 Fluid motion

Now that we have described the forces at play in a fluid and the conditions for equilibrium, let's focus on fluid motion.

1.4.1 Equation for momentum conservation

Momentum conservation for a fluid domain simply follows from Newton's second law $m\boldsymbol{\gamma} = \Sigma\boldsymbol{F}$, never forget this! Let's write this law for a material domain $V(t)$, using index notation:

$$\frac{d}{dt} \iiint_{V_{\text{mat}}} \rho u_i dV = \oint_{\partial V_{\text{mat}}} \sigma_{ij} n_j dS + \iiint_{V_{\text{mat}}} \rho f_i dV \quad (1.40)$$

or, going to the local level:

$$\rho \frac{du_i}{dt} = \frac{\partial \sigma_{ij}}{\partial x_j} + \rho f_i \quad (1.41)$$

That was quite simple. However there is a loophole in the previous expression as the stress tensor $\boldsymbol{\sigma}$ is here unknown (except in the case of limited interest of a static fluid, see equation (1.25)). Even if equation (1.41) holds true whatever the nature of the fluid (even for say exotic viscoelastic fluids), it is of limited use as long as this stress tensor is not clarified. We therefore have to make a connection between the stresses and the motion of the fluid, for we expect that the stresses will change as soon as the fluid starts to flow. This connection will be made thanks to *constitutive laws* that will really characterise the fluid we are looking at.

1.4.2 Energy conservation

The energy of a fluid particle is composed of a macroscopic kinetic energy $\frac{1}{2}\rho\mathbf{u}^2$ and a remainder, that encompasses in particular the microscopic (or *thermal*) kinetic energy of molecules, in the form of the *internal energy* e . The first principle of thermodynamics states that this energy varies when external forces exert a work, and when there is an input or output of internal energy (i.e. *heat*) through the boundaries:

$$\frac{d}{dt} \iiint_{V_{\text{mat}}} \left(\frac{1}{2}\rho u^2 + \rho e \right) dV = \oint_{\partial V_{\text{mat}}} (\boldsymbol{\sigma} \cdot \mathbf{n}) \cdot \mathbf{u} dS + \iiint_{V_{\text{mat}}} \rho \mathbf{f} \cdot \mathbf{u} dV - \oint_{\partial V_{\text{mat}}} \mathbf{q} \cdot \mathbf{n} dS. \quad (1.42)$$

This equation can be rewritten at the fluid particle scale:

$$\rho \frac{d}{dt} \left(\frac{1}{2}u^2 + e \right) = \nabla \cdot (\boldsymbol{\sigma} \cdot \mathbf{u}) + \rho \mathbf{f} \cdot \mathbf{u} - \nabla \cdot \mathbf{q}. \quad (1.43)$$

As written, this balance mixes macroscopic and microscopic energies. It is however possible to disentangle these two contributions by multiplying Cauchy's equation (1.41) with \mathbf{u} to get:

$$\rho \frac{d}{dt} \left(\frac{1}{2}u^2 \right) = (\nabla \cdot \boldsymbol{\sigma}) \cdot \mathbf{u} + \rho \mathbf{f} \cdot \mathbf{u}. \quad (1.44)$$

¹⁰This is a really crude approximation on the density profile, which better describes incompressible (!) planets rather than gaseous ones or stars. The hydrostatics of stars can however be rationalised by taking into account the state law of polytropes, and possibly the radiation pressure adding up to the kinetic pressure. The reader interested in stellar hydrostatics may look at the *Lane-Emden equation* described e.g. in Chandrasekhar (1957, chap. IV).

On subtracting these last two equations, we obtain an equation for the evolution of the internal energy e alone:

$$\rho \frac{de}{dt} = \boldsymbol{\sigma} : \mathbf{D} - \nabla \cdot \mathbf{q}. \quad (1.45)$$

Here, \mathbf{D} is the symmetric part of the velocity gradient:

$$D_{i,j} = \frac{1}{2} \left(\frac{\partial u_i}{\partial x_j} + \frac{\partial u_j}{\partial x_i} \right). \quad (1.46)$$

We can express energy conservation in a more convenient form, let's first remark that fluid particles are exposed to neighbouring fluid (i.e. are not encased in rigid boxes). For such systems exposed to the open world, thermodynamicists have developed a clever way to account for energy variations without having to worry about the work done during expansion or contraction, by introducing the concept of *enthalpy* (Atkins, 2010), defined¹¹ as $h = e + p/\rho$. Reexpressing equation (1.45) with enthalpy we get:

$$\rho \frac{dh}{dt} = \boldsymbol{\sigma} : \mathbf{D} - \nabla \cdot \mathbf{q} + \frac{dp}{dt} + p (\nabla \cdot \mathbf{u}). \quad (1.47)$$

A connection between enthalpy (or internal energy) and the state variables p and T (the temperature) can be obtained if we suppose that, locally, the fluid particle reaches thermodynamical equilibrium:

$$dh = c_p dT + \frac{1}{\rho} (1 - \alpha T) dp, \quad (1.48)$$

where c_p denotes the specific heat capacity at constant pressure and $\alpha = \rho (\partial (1/\rho) / \partial T)_p$ the thermal expansion coefficient¹². Following the fluid particle in its motion, we get the following expression for the rate of variation of specific enthalpy:

$$\rho \frac{dh}{dt} = \rho c_p \frac{dT}{dt} + \left(1 + \frac{T}{\rho} \left(\frac{\partial \rho}{\partial T} \right)_p \right) \frac{dp}{dt}. \quad (1.49)$$

¹¹Note that we here use the *specific* enthalpy, that is the enthalpy per unit mass.

¹²To obtain this relation we may start from the enthalpy differential:

$$dH = \underbrace{dU + p dV}_{T dS} + V dp,$$

where we have used $T dS = dU + p dV$ as a defining relation for entropy. Expressing the total differential of entropy as a function the state variables differentials dp and dT we get:

$$dH = T \left(\left(\frac{\partial S}{\partial T} \right)_p dT + \left(\frac{\partial S}{\partial p} \right)_T dp \right) + V dp.$$

To make further progress we note that the definition of the heat of capacity at constant pressure is $C_p \equiv (\partial H / \partial T)_p$ and make use of Maxwell relations to express the entropy derivative as a derivative of the volume. To do so, we write the total differential of Gibbs energy:

$$dG = -SdT + Vdp,$$

and deduce the following Maxwell relation:

$$-\left(\frac{\partial S}{\partial p} \right)_T = \left(\frac{\partial V}{\partial T} \right)_p \equiv V\alpha.$$

With the help of this last relation we may rewrite the enthalpy differential as:

$$dH = C_p dT + V (1 - \alpha T) dp.$$

If V denotes the volume of a fluid particle, we can divide this last relation by its mass to obtain the desired result.

This expression allows us to get the following form for energy conservation at the local level:

$$\rho c_p \frac{dT}{dt} = \underbrace{\boldsymbol{\sigma} : \mathbf{D} + p(\nabla \cdot \mathbf{u})}_{\text{viscous dissipation}} - \nabla \cdot \mathbf{q} - \frac{T}{\rho} \left(\frac{\partial \rho}{\partial T} \right)_p \frac{dp}{dt}. \quad (1.50)$$

In equation (1.45), $\boldsymbol{\sigma} : \mathbf{D} + p(\nabla \cdot \mathbf{u})$ corresponds to a macroscopic energy transfer into internal energy, and can be shown to be a strictly positive quantity (e.g. Leal, 2007). From a macroscopic perspective, this means that kinetic energy has been lost into “heat”, and for this reason this term is referred to as **viscous dissipation**.

1.5 Constitutive laws

The conservation laws expressed for a flowing fluid are expressed with fluxes and stresses whose precise form still remains to be determined. In order to make some progress in this determination, let's consider the following situation: without any macroscopic motion, a liquid contains a colourant with concentration c distributed inhomogeneously, with area more or less concentrated. Even in absence of a mean motion, the collisions between molecules will lead the colourant molecules to migrate randomly in the liquid. As a result, due to the inhomogeneous colourant distribution, there will be an excess of particles traversing δA that originate from a more concentrated area than the reverse. The consequence is a net transport of colourant molecules from more concentrated area to less concentrated ones, that will be active as long as the non-equilibrium situation persists: this is the **diffusion process**. It seems difficult to track the motion of each colourant particles from a statistical viewpoint. But from a *phenomenological* viewpoint, it is quite clear that diffusion will remain active only if a concentration gradient ∇c exists. The idea of **gradient-type laws** is to suppose that the components of the flux \mathbf{j}_{diff} depend linearly on ∇c , i.e. :

$$(\mathbf{j}_{\text{diff}})_i = k_{ij} \frac{\partial c}{\partial x_j}. \quad (1.51)$$

For an isotropic fluid, it seems reasonable to consider that in absence of any privileged axes the flux will be aligned with ∇c and of opposite sign (so as to restore equilibrium rather than to destroy it further!), so that :

$$\mathbf{j}_{\text{diff}} = -k \nabla c, \quad (1.52)$$

and therefore:

$$k_{ij} = -k \delta_{ij}. \quad (1.53)$$

We here recover the general form of mass (Fick) and energy (Fourier) transport:

$$\begin{cases} \text{Fick's law :} & \mathbf{j}_{\text{mass}} = -D \nabla c \\ \text{Fourier's law :} & \mathbf{j}_{\text{energy}} = -k \nabla T \end{cases} \quad (1.54)$$

$$(1.55)$$

▷ **Momentum diffusion and viscous stress.** The case of momentum diffusion is a bit more complex due to the vectorial nature of $\rho \mathbf{u}$. To start with let's consider the simple situation of a parallel flow $(U(y), 0, 0)$. Due to intermolecular collisions, there is a vertical **diffusion** of momentum. As for mass transport, we suppose that the flux is linear with the momentum gradient, so that:

$$\mathbf{j}_{\text{diff}} = -\mu \frac{dU}{dy}, \quad (1.56)$$

Note that this vertical flux of horizontal momentum has the following dimensions;

momentum per unit volume \times volume/area/time

or $[ML^{-1}T^{-2}]$, the same dimension of a stress. This dimensional similitude is no coincidence: the transferred momentum is achieved with a stress, in accordance with Newton's second law. We may indeed rewrite (1.56) as:

$$\sigma_{xy} = \mu \frac{dU}{dy}, \quad (1.57)$$

which is the horizontal stress exerted on a surface with a vertical normal¹³. The proportionality coefficient μ characterising the efficiency of momentum transport is the *dynamic viscosity*.

▷ **General expression for the stress tensor of a Newtonian fluid.** In the context of a general flow, we can foresee that the stress tensor will depend on each component of the velocity gradient¹⁴, so that:

$$\sigma_{ij} = -p \delta_{ij} + \alpha_{ijkl} \frac{\partial u_k}{\partial x_l}. \quad (1.58)$$

This form of the stress tensor is compatible with the static fluid stress tensor presented earlier: as soon as the velocity vanishes, the stress tensor adopts its static limit (1.25). But we can go further. If we decompose the velocity gradient tensor into a symmetric part D (associated with a deformation) and an antisymmetric part ω (associated with solid body rotation) :

$$u_{i,j} = D_{i,j} + \omega_{i,j} \quad \text{with} \quad D_{i,j} = \frac{1}{2} \left(\frac{\partial u_i}{\partial x_j} + \frac{\partial u_j}{\partial x_i} \right) \quad \text{et} \quad \omega_{i,j} = \frac{1}{2} \left(\frac{\partial u_i}{\partial x_j} - \frac{\partial u_j}{\partial x_i} \right),$$

Actually momentum diffusion (i.e. viscous stress) can only occur when the flow deviates from solid-body motion (translation or rotation): as a result σ cannot depend on ω and:

$$\sigma_{ij} = -p \delta_{ij} + A_{ijkl} D_{kl}. \quad (1.59)$$

Additional considerations on the fluid isotropy that we will not develop here allow for a drastic reduction in the number of coefficients to finally get:

$$\sigma_{ij} = -p \delta_{ij} + 2\mu D_{ij} + \lambda (\nabla \cdot \mathbf{u}) \delta_{ij}. \quad (1.60)$$

1.6 Wrapping up: The Navier-Stokes and energy equations

1.6.1 The Navier-Stokes equation

Having elucidated the structure of the stress tensor (1.60) we can rewrite the equation for momentum conservation (1.41) :

$$\rho \frac{du_i}{dt} = \rho f_i - \frac{\partial p}{\partial x_i} + \frac{\partial}{\partial x_j} (2\mu D_{ij} + \lambda (\nabla \cdot \mathbf{u}) \delta_{ij}) \quad (1.61)$$

This equation is the *Navier-Stokes equation*.

In the particular case (but of great practical interest) of an incompressible evolution with viscosity gradient, this equation simplifies to:

$$\rho \frac{du_i}{dt} = \rho f_i - \frac{\partial p}{\partial x_i} + \mu \frac{\partial^2 u_i}{\partial x_j \partial x_j}, \quad (1.62)$$

or, in vectorial form:

$$\underbrace{\rho \left(\frac{\partial \mathbf{u}}{\partial t} + (\mathbf{u} \cdot \nabla) \mathbf{u} \right)}_{m\gamma} = \underbrace{-\nabla p + \mu \nabla^2 \mathbf{u} + \rho \mathbf{f}}_{\Sigma F}. \quad (1.63)$$

¹³the reader will note the sign difference between the expressions (1.56) and (1.57) that originate from the notation convention for stresses.

¹⁴This is this linear dependence to shear that qualifies a fluid as Newtonian. But we can imagine (and actually there exists) more complex relations, of nonlinear nature, between stress and shear. **Rheology** is the discipline that studies these particular non-newtonian behaviours.

1.6.2 The energy equation

Similarly, rewriting the general form for energy conservation (1.50) for a Newtonian fluid we get:

$$\rho c_p \frac{dT}{dt} = \underbrace{2\mu \mathbf{D} : \mathbf{D}}_{\text{dissipation}} + \nabla \cdot (k \nabla T) - \frac{T}{\rho} \left(\frac{\partial \rho}{\partial T} \right)_p \frac{dp}{dt}. \quad (1.64)$$

It can be noted here that the viscous dissipation term takes the very simple form $2\mu \mathbf{D} : \mathbf{D}$. Finally, we remark that the last term in the right hand side is usually neglected in practical applications; even in configurations where dp/dt is not strictly zero, the weak variation of the density with temperature $(\partial \rho / \partial T)_p$ for usual fluids makes this term negligible in front of the other contributions.

Chapter 2

Boundary conditions and interfaces

We have seen in the previous chapter how to express mass, momentum and energy conservation at the fluid particle level, and we have derived the corresponding equations for fluid motion. These equations are naturally associated with **boundary conditions** that either express conservation laws (e.g. no mass flux at a boundary) or peculiar physical processes occurring at a surface (temperature or velocity continuity). In both cases these boundary conditions will be pivoting in the determination of the solution.

One striking experimental demonstration of this coupling between the large and the small is provided Fig. 2.1, where two seemingly identical spheres impacting water at the same speed either enter the pool very smoothly or by creating a considerable splash. Actually the difference between the two spheres is a nanometre-thick coating making the sphere either hydrophilic or hydrophobic, thereby revealing how nanometric effects at the boundary can influence large-scale hydrodynamics (Duez *et al.*, 2007; Eggers, 2007).



Figure 2.1: Left: a hydrophilic sphere impacts water without creating any significant disturbance. Right: a similar sphere with a nanometre-thick hydrophobic coating creates a significant splash on impact (Duez *et al.*, 2007).

We now review the different types of boundary conditions that fluids satisfy at boundaries.

2.1 Fluxes at boundaries: impermeability and imbibition

Let's consider a solid moving in a fluid at velocity \mathbf{u}_s (possibly time dependent) and let's conduct a mass balance on a small cylindrical volume of base δA and height δh located across the fluid and the solid (Fig. 2.2). Now let δh tends to 0 so that the mass element shrinks down to zero. From now on, the mass variation of the element should necessarily be zero, and this implies

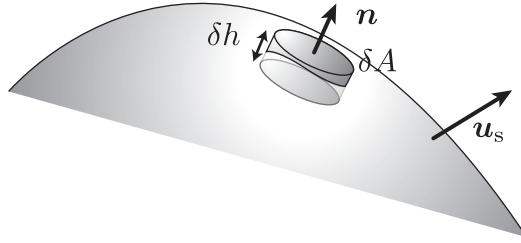


Figure 2.2: Balance over an elementary volume located across a solid boundary.

that the mass flux from the fluid has to be balanced by the mass flux from the solid side:

$$-(\mathbf{j}_{\text{fluid}} \cdot \mathbf{n}_{\text{fluid}}) \delta A - (\mathbf{j}_{\text{solid}} \cdot \mathbf{n}_{\text{solid}}) \delta A = 0. \quad (2.1)$$

Let's write arbitrarily $\mathbf{n} = \mathbf{n}_{\text{fluid}} = -\mathbf{n}_{\text{solid}}$ so that:

$$-\mathbf{j}_{\text{fluid}} \cdot \mathbf{n} + \mathbf{j}_{\text{solid}} \cdot \mathbf{n} = 0. \quad (2.2)$$

In absence of fluid mixing phenomena, the fluid velocity \mathbf{u} already takes into account diffusive effects (it is the chemical species velocity) and the mass flux reduces to the convective flux. Beware that as we are in the solid reference frame, the relative velocity of the fluid is $\mathbf{u} - \mathbf{u}_s$, so that the mass flux on the fluid side is:

$$\mathbf{j}_{\text{fluid}} = \rho (\mathbf{u} - \mathbf{u}_s). \quad (2.3)$$

▷ **The impermeable wall.** A very common case is that of an **impermeable** solid in which the fluid cannot penetrate; the fluid mass flux within the solid is therefore zero and $\mathbf{j}_{\text{solid}} = 0$. Mass conservation expressed at an impermeable boundary therefore reduces to:

$$\mathbf{u} \cdot \mathbf{n} = \mathbf{u}_s \cdot \mathbf{n} \quad (2.4)$$

This is the **impermeability condition** for an object (or a wall). As the name implies, it simply expresses the fact that the fluid cannot penetrate into the solid. This condition takes the form of a **continuity of normal velocities**.

Note: in the quite particular (but still very common!) case of a fixed solid object, this condition reduces to $\mathbf{u} \cdot \mathbf{n} = 0$.

▷ **Permeable wall.** The previous discussion naturally extends to the case of permeable walls. Those may correspond to biological tissues permeable to given solutes, to materials swollen by solvents, to terrains soaked by rain or to lifting sails or wings made porous in order to control the boundary layer (such as Cousteau and Malavard' turbosail seen in the lecture, see also Fig. 2.3).

Now the mass flux is non-zero and its precise determination requires a knowledge of the flow *inside* the solid. Suppose however that the imbibition velocity $\mathbf{u}_{\text{imbib}}$ be constant and known (this corresponds for example to a suction with an imposed flowrate). The mass conservation at the permeable wall will then be written:

$$\rho(\mathbf{u} - \mathbf{u}_s) \cdot \mathbf{n} = \rho(\mathbf{u}_{\text{imbib}}) \cdot \mathbf{n}, \quad (2.5)$$

thus

$$\mathbf{u} \cdot \mathbf{n} = (\mathbf{u}_s + \mathbf{u}_{\text{imbib}}) \cdot \mathbf{n}. \quad (2.6)$$

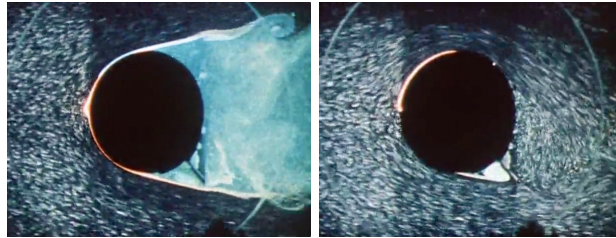


Figure 2.3: Left: A cylinder placed in a crossflow exhibits a wide wake, associated with an important inertial drag force. Right: with an appropriate suction on the cylinder' surface, the flow reattaches and a significant lift is now obtained. This is the underlying principle of the **turbosail**. Experiments performed in Malavard's lab at ONERA (excerpt from the movie *Écoulements tourbillonnaires d'une maquette de turbovoile - 1984*).

▷ **Boundary conditions on a concentration field near a wall.** The boundary conditions to apply on the transport equation of a concentration field (1.21) can be obtained following the same principles. Imagine a concentration field transported with a fluid flow \mathbf{u} . Suppose also that an (impermeable) solid is moving in the fluid at velocity \mathbf{u}_s . In the solid reference frame the mass flux across any surface $\delta A \mathbf{n}$ is:

$$\mathbf{j}_{\text{mass}} = \mathbf{j}_{\text{conv}} + \mathbf{j}_{\text{diff}} = c(\mathbf{u} - \mathbf{u}_s) - D\nabla c. \quad (2.7)$$

The impermeability condition at the wall for the concentration field c is therefore:

$$c(\mathbf{u} - \mathbf{u}_s) \cdot \mathbf{n} - D\nabla c \cdot \mathbf{n} = 0, \quad (2.8)$$

because the mass flux inside the solid is zero. On using the impermeability condition on the velocity field (2.4), this relation reduces to:

$$\nabla c \cdot \mathbf{n} \equiv \frac{\partial c}{\partial n} = 0. \quad (2.9)$$

This Neumann condition is also called a **no-flux boundary condition**.

▷ **Mass transfer at an interface: evaporation.** One last example of boundary conditions arising from conservation considerations is the continuity of the mass flux across a liquid-gas interface, when the (single-phase) liquid is evaporating.

Let's write a mass balance on a fluid element analogous to the previous one: a small cylindrical element of base δA and height δh located across a moving interface with velocity \mathbf{u}_i . We let the height δh of the element tend to zero, so that the element mass equally tends to zero. The mass balance over this element is:

$$\mathbf{j}_{\text{liquid conv.}} \cdot \mathbf{n} = (\mathbf{j}_{\text{gas conv.}} + \mathbf{j}_{\text{gas diff.}}) \cdot \mathbf{n} \quad (2.10)$$

so that :

$$\underbrace{\rho_\ell (\mathbf{u}_\ell - \mathbf{u}_i) \cdot \mathbf{n}}_{\text{interface ablation}} = \underbrace{\rho_v (\mathbf{u}_g - \mathbf{u}_i) \cdot \mathbf{n}}_{\text{Stefan's flow}} - \underbrace{D\nabla \rho_v \cdot \mathbf{n}}_{\text{diffusive mass flux}}. \quad (2.11)$$

From this balance it is apparent that the interface evaporation is driven by two contributions: a convective mass flux and a diffusive one. The convective (so-called *Stefan*) flow results from the expansion of liquid solvent into vapour solvent. In the context of a violent evaporation (e.g. boiling, combustion front), this is the dominating contribution and from the balance relation we see that in this context:

$$\|\mathbf{u}_g\| \sim \underbrace{\frac{\rho_\ell}{\rho_v}}_{\gg 1} \|\mathbf{u}_i\|.$$

However in the other limit where evaporation is very slow, which corresponds to everyday life situations, such as the slow drying of a water drop in plain air, this is the reverse. The diffusive mass flux largely overrides the convective (Stefan) flux, so that it can safely be disregarded¹⁵.

▷ **Application: drop evaporation and D²-law.** We can build up on the previous considerations to provide with an estimate of the time it takes for an isolated and still water drop to evaporate in plain air. At first sight, we might be tempted to scale the overall mass loss rate of the drop with its surface $\propto R^2$, and conclude that the radius of the drop decreases linearly with time. However this is not so, because the diffusive transport of water away from the drop sets a bound on how fast the drop evaporates: drop evaporation is an example of a **diffusion-limited** problem. Drop evaporation in still air was first investigated by Maxwell (1890) who was interested in developing a theory of the wet bulb thermometer – a curious and ingenious device aimed at measuring air humidity. Langmuir (1918) obtained the very same result years later, without apparent knowledge of Maxwell's former investigations.

Considering a still drop with no motion at constant temperature¹⁶, we can rewrite the boundary condition (2.11) at the surface of the drop as:

$$\rho_\ell \frac{dR}{dt} = D \frac{\partial c}{\partial r} \Big|_{r=R}. \quad (2.12)$$

Here we neglected Stefan's flow contribution, and benefited from the spherical symmetry of the problem to project it along e_r . The velocity of the interface has been replaced with the rate of variation of R , and we have denoted c the water vapour concentration, and D its diffusion coefficient in air. It is apparent from this expression that R is directly driven by the vapour density profile in air, which itself is set by diffusion. Introducing air's humidity \mathcal{H} such that $c = c_{\text{sat}} \mathcal{H}$, we may also rewrite this boundary condition as:

$$\frac{dR}{dt} = D \frac{c_{\text{sat}}}{\rho_\ell} \frac{\partial \mathcal{H}}{\partial r} \Big|_{r=R}. \quad (2.13)$$

Humidity is a dimensionless quantity equal to 1 at the drop' surface, and 0 in dry air (typically this is the value at infinity). To make progress, it is therefore necessary to look at the diffusion equation for the water vapour:

$$\frac{\partial \mathcal{H}}{\partial t} = D \frac{1}{r} \frac{\partial^2}{\partial r^2} (r \mathcal{H}). \quad (2.14)$$

A quick order of magnitude estimate for the diffusion profile build-up reads:

$$\tau_{\text{diff}} \sim R^2 / D,$$

as pure dimensional analysis could have revealed immediately. This characteristic timescale may conveniently be compared to the drop evaporation timescale, estimated with an order of magnitude analysis from (2.13):

$$\frac{R}{\tau_{\text{evap}}} \sim D \frac{c_{\text{sat}}}{\rho_\ell} \frac{\Delta \mathcal{H}}{R}. \quad (2.15)$$

Here $\Delta \mathcal{H}$ is typically of order 1. Rearranging we have:

$$\frac{\tau_{\text{diff}}}{\tau_{\text{evap}}} \sim \frac{c_{\text{sat}}}{\rho_\ell}.$$

¹⁵It can be shown that the ratio between Stefan over diffusive flow is simply the mass fraction of solvent in the gas near the interface (Magdelaine, 2019). When a liquid is boiling, the air surrounding the interface is pure solvent vapour, so this mass fraction is of order 1 and Stefan's flow contribution becomes important. Conversely, the saturation vapour pressure of water at ambient temperature is 2.3 kPa – corresponding to a mass fraction of water vapour in air of 1.5 %. In this limit, the contribution of Stefan's flow is negligible to describe evaporation.

¹⁶This is arguably a fragile hypothesis, as the enthalpy of evaporation is responsible for an overall cooling down of the drop. While D^2 's law is found to hold, the prefactor of the law becomes non-trivial when taking all effects into account, see Cazabat & Guena (2010) for a discussion.

For water in air at ambient temperature, $c_{\text{sat}} = 1.7 \times 10^{-2} \text{ kg/m}^3$, whereas $\rho_\ell = 1000 \text{ kg/m}^3$. This indicates that evaporation is very slow with regards to diffusion build-up: the water vapour profile adjusts almost instantaneously as the drop shrinks. This justifies the search of a steady-state water vapour profile for (2.14):

$$\mathcal{H}(r) = \frac{R}{r} \Delta \mathcal{H} + \mathcal{H}_\infty, \quad (2.16)$$

with $\Delta \mathcal{H} = 1 - \mathcal{H}_\infty$. This humidity field allows to rewrite (2.13) as:

$$\frac{dR}{dt} = -D \frac{c_{\text{sat}}}{\rho_\ell} \frac{\Delta \mathcal{H}}{R}, \quad (2.17)$$

from which we obtain the radius evolution:

$$R(t) = \left(R_0^2 - 2D \frac{c_{\text{sat}}}{\rho_\ell} \Delta \mathcal{H} t \right)^{1/2}, \quad (2.18)$$

a result known as *D²-law of evaporation* (so called because the diameter squared of the drop decreases linearly with time). The timescale of an isolated, evaporating droplet follows:

$$\tau_{\text{evap}} = \frac{1}{2} \frac{R_0^2}{D} \frac{\rho_\ell}{c_{\text{sat}}} \frac{1}{\Delta \mathcal{H}}, \quad (2.19)$$

a result consistent with our quick order of analysis estimate (2.15).

2.2 Phenomenological conditions: adherence and continuity

In addition to the previous boundary conditions arising from conservation principles, fluids are also subject to other boundary conditions as well. The latter have been established and confirmed on experimental grounds, so there is a consensus about their relevance but not an exact demonstration. These phenomenological conditions are **field continuity conditions** at interfaces and apply on velocity, temperature etc.

▷ **A short history of adherence.** The adherence condition $\mathbf{u} = \mathbf{u}_s$ has an astonishing history full of twists and turns, which is accounted for in details in Goldstein (1950). At the XVIIIth century, the theoretical description of potential flows (corresponding to the idealisation of perfect flow of fluid) was already well established, but the comparisons with experimental data were mediocre. Daniel Bernoulli was well aware of this fact and attributed the discrepancies between (ideal) predicted flows and those observed to some “adherence condition” that would prevail at the wall. Coulomb then demonstrated experimentally that a disk oscillating in a liquid was not particularly affected by a change in surface properties (smooth, rough or covered with grease). Therefore it appeared to Coulomb that the fluid velocity matched the disk velocity in its vicinity. In this vision the fluid has the same properties in every point of space; the flow just fulfills an additional condition at the wall.

But during the XIXth century alternate theories appeared. Girard proposed that the liquid layer adjacent to a wall had differing physical properties, leading it to adhere the solid. The next fluid layer (composed of “regular fluid”) could then freely slip onto the first affixed layer. Navier also got interested into this problem and suggested a boundary condition involving a slip directly proportional to the shear stress $\beta u = \mu \frac{\partial u}{\partial n}$. Here the ratio μ/β has the dimension of a length: it is the *slip length*. From there a period of relative confusion ensued where famous theoreticians of the time (Poisson, Stokes) alternately adopted one or the other of the boundary conditions. With time however, delicate experiments conducted by Couette or Maxwell advocated definitely for the adherence condition. Maxwell suggested on molecular dynamics considerations that if

Navier's condition was effectively valid, the length over which slip occurred was so small – of the order of a few mean free paths – that considering it to be zero was a really reasonable hypothesis. This amounted to consider adherence at the wall: $\mathbf{u} = \mathbf{u}_s$ (Maxwell, 1879). This is in particular verified in the usual conditions of laboratory experiments, but not necessarily for rarefied gas flows (e.g. atmospheric reentry, hypersonic flight) or flows involving fluids with long polymer chains (microfluidic flows), as experiments confirm (Hénot *et al.*, 2018).

During the xxth century, the almost perfect agreement between experimental observations and theoretical predictions using adherence condition for a number of flows (Poiseuille flow, Couette flow, Stokes' sphere settlement in a viscous fluid, the instability threshold for the Taylor-Couette experiment etc) definitely settled the validity of this condition.

Moreover, the scaling laws for the drag on an object deduced from dimensional considerations based on the characteristic scales ρ, U, D and μ capture the evolution of aerodynamic forces over a wide range of scales. If another lengthscale (associated with slip) was relevant in the description of conventional flows, it would result in an alteration of the scaling laws (not observed).

We can understand adherence condition (continuity of \mathbf{u} across an interface) but also the condition on temperature continuity as resulting from equilibrium at the molecular level. The extremely rapid transfers between neighbouring molecules induce a quasi-instantaneous equilibrium of mean momentum (velocity) and mean thermal agitation velocity (temperature) (Batchelor, 1967). At an interface between a medium I and a medium II (solid-fluid, or fluid-fluid), we will therefore get:

$$\mathbf{u}_I = \mathbf{u}_{II} \quad \text{and} \quad T_I = T_{II}. \quad (2.20)$$

2.3 Where is the interface?

A wide range of flows are associated with interfaces: avalanches, rivers, oceans, emulsion droplets, rain or ink drops etc. As we shall see, an interface between a liquid and another fluid is not just an immaterial boundary geometrically delimiting portions of space occupied by fluids. An interface is an **active region** where surface tension forces act, in some way analogous to those exerted by a taut membrane.

But before precising the nature of these forces acting on the interface, we first need to be able to know where the interface is! Indeed, an interface is constantly moving by definition and we have to start tracking the interface through time and space. This is the purpose of the *kinematic boundary condition* which will allow us to follow the interface in its motion.

2.3.1 Kinematic boundary condition.

In order to describe the motion of any given interface, as a free surface for example, let's introduce an arbitrary function $\mathcal{S}(\mathbf{x}, t)$ that vanishes on the interface at all times: for each point $\mathbf{x}_{\text{interf}}$ of the interface, $\mathcal{S}(\mathbf{x}_{\text{interf}}, t) = 0$. Between two successive instants, an interface point is displaced with a distance $\delta\mathbf{x} = \mathbf{u}_i \delta t$ and:

$$\mathcal{S}(\mathbf{x}_{\text{interf}} + \mathbf{u}_i \delta t, t + \delta t) \approx \underbrace{\mathcal{S}(\mathbf{x}_{\text{interf}}, t)}_0 + \delta t \underbrace{\left(\frac{\partial \mathcal{S}}{\partial t} + (\mathbf{u}_i \cdot \nabla) \mathcal{S} \right)}_{\frac{d_i \mathcal{S}}{dt}} = 0. \quad (2.21)$$

To get the interface velocity \mathbf{u}_i ¹⁷ we just need to express the mass flux boundary condition at the interface. If there is no mass transfer at the interface (such as e.g. evaporation), the latter reads:

$$\rho(\mathbf{u} - \mathbf{u}_i) \cdot \mathbf{n} = 0 \quad \text{thus} \quad \mathbf{u} \cdot \mathbf{n} = \mathbf{u}_i \cdot \mathbf{n}, \quad (2.22)$$

¹⁷We note that in the expression of \mathcal{S} , only the normal component $\mathbf{u}_i \cdot \mathbf{n}$ of \mathbf{u}_i at the interface is involved.

so that the kinematic boundary condition describing the motion of a free surface simply reads:

$$\frac{d\mathcal{S}}{dt} = 0 \quad (2.23)$$

▷ **Example: description of a free surface.** Consider a free surface such as the ocean's, characterised¹⁸ with $z = \zeta(x, y, t)$. The surface is described at each instant by the vanishing of the function¹⁹ :

$$\mathcal{S}(\mathbf{x}, t) = z - \zeta(x, y, t). \quad (2.24)$$

The kinematic boundary condition describing the position of the free surface is therefore:

$$\frac{d\mathcal{S}}{dt} = 0 \quad \text{hence} \quad \frac{\partial \zeta}{\partial t} = u_z - u_x \frac{\partial \zeta}{\partial x} - u_y \frac{\partial \zeta}{\partial y} \quad (2.25)$$

2.3.2 Surface geometry I. Normals.

In a number of problems involving free surfaces, deformable and/or complex boundaries, the expression for the normal vector has to be provided. A systematic procedure to obtain the expression for this vector stems in remarking that the free surface coincides with a \mathcal{S} -isosurface. As a result the normal vector is necessarily parallel with the **gradient** of \mathcal{S} :

$$\mathbf{n} = \frac{\nabla \mathcal{S}}{\|\nabla \mathcal{S}\|} \quad (2.26)$$

▷ **Example: free surface normal.** Let's consider the previous example again. We have:

$$\nabla \mathcal{S} = \begin{pmatrix} -\frac{\partial \zeta}{\partial x} \\ -\frac{\partial \zeta}{\partial y} \\ 1 \end{pmatrix},$$

so

$$\mathbf{n} = \frac{1}{\sqrt{1 + \left(\frac{\partial \zeta}{\partial x}\right)^2 + \left(\frac{\partial \zeta}{\partial y}\right)^2}} \begin{pmatrix} -\frac{\partial \zeta}{\partial x} \\ -\frac{\partial \zeta}{\partial y} \\ 1 \end{pmatrix}. \quad (2.27)$$

We note the the direction of this normal is quite arbitrary and chosen by convention (usually, the convention is that of exterior-pointing normal. However this only makes sense if the very notion of exterior makes sense!).

2.4 Capillarity

Having described kinematically interfaces (i.e. how to locate them) along with the boundary conditions resulting from mass conservation and molecular equilibria (adherence condition), we shall now get interested into the dynamical aspects of interfaces and more particularly to the phenomenon of *capillarity* (de Gennes *et al.*, 2015).

An interface between two immiscible fluids, as that between air and water is, is a material surface separating the two media. But actually such an interface is in reality way more than a simple geometric place delimiting two portions of space. An interface **bears forces** whose manifestation is visible in daily-life examples, such as the clogging of wet hairs, the spooling of spider thread within glue droplets or the sustentation of small aquatic animals such as the Gerris (Fig. 2.4).

¹⁸We here suppose that the interface is single valued (no wave breaking!).

¹⁹We could imagine other functions as well, e.g. $\mathcal{S}(\mathbf{x}, t) = \tanh(z - \zeta(x, y, t)) \dots$

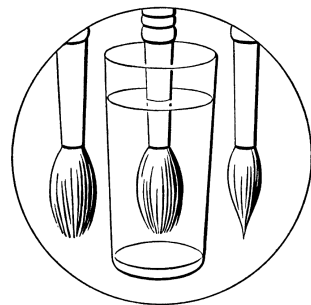


Fig. 1

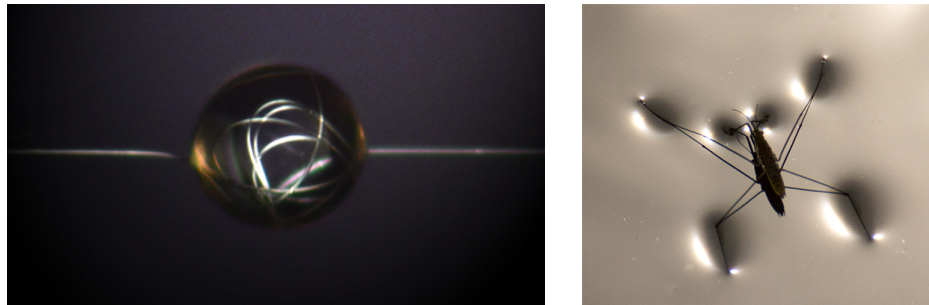


Figure 2.4: Top: when pulled out of water, a wet brush has its bristles stuck altogether, but those are neatly separated is the brush is dry or fully immersed (Boys, 1890). Bottom left: a drop deposited on a sufficiently thin fibre such as the spider capture silk induces coiling and spooling within the droplet (Elettro *et al.*, 2016). Bottom right: the Gerris, an aquatic insect, can literally walk on water although it is denser ([photograph by Ryoichi on Flickr](#)). These examples are manifestations of surface tension exerted at liquid-gas interfaces.

2.4.1 Cohesion

The microscopic origin of surface tension is rooted in **cohesion** effects in liquids. Indeed, atoms or molecules that constitute matter interact with each other with forces of changing nature. Repulsive at very short distance, the forces become attractive at longer range. In the context of a gas, the intermolecular distances are far too large for these interactions to have any notable effect. But this is not true for dense phases such as liquids where molecules attract each other. This matter cohesion phenomenon is responsible for the rounded shape of droplets, the curvature of menisci or that of soap films. The history of the link between attractive forces and surface tension is already present in the writings of Newton, but this link was not really elucidated until Laplace in 1805 (de Laplace, 1805). With the unique hypothesis of attractive forces between two matter particles decaying with distance, Laplace succeeded in finding with differential calculus all equilibria shapes of interfaces. He also explained the capillary rise in tubes, a phenomenon resisting understanding so far (Rowlinson, 2005). He further evidenced a pressure jump phenomenon (normal stress) proportional to curvature, as we shall now see.

2.4.2 Surface tension

In parallel to Laplace's works on cohesion and capillarity, Thomas Young also managed to find in 1805 a result on the pressure jump across interfaces identical to Laplace's finding. But he followed an entirely different route (Young, 1805). On the basis of experimental observations of free surface deformations similar to those of elastic membrane, Young postulated the existence of a tension force localised at the liquid surface, and analogue to membrane tension – such as the one developing in a stretched balloon. Following this reasoning, a small, flat and rectangular surface element $\delta S = \delta\ell_1\delta\ell_2$ such as the one illustrated figure 2.5 would be subject to a total force:

$$(\gamma\delta\ell_2 - \gamma\delta\ell_1)\mathbf{e}_1 + (\gamma\delta\ell_1 - \gamma\delta\ell_2)\mathbf{e}_2 = 0.$$

As a matter of fact, each force contribution is balanced by another because the surface is flat. But we feel here that this result may change as soon as the surface will be curved. Before proceeding in the estimation of the surface tension force for a general surface, we have to characterise the curvature of a surface.

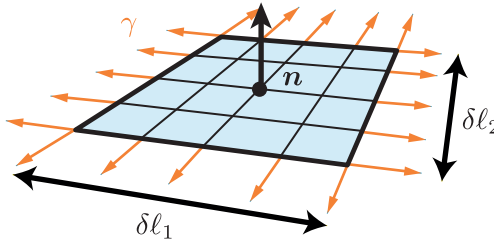


Figure 2.5: A flat interface portion is subject to a tension force at its periphery.

2.4.3 Surface geometry II. Curvature.

Let's consider the portion of curved interface represented figure 2.6. The curvature of the surface on a given point is a geometric quantity that can be built as follows. Start by identifying the normal \mathbf{n} to the surface at the chosen point. Consider now two perpendicular planes that each contain \mathbf{n} . Each plane will intersect the surface following a curve which may be approximated by a circle in the vicinity of the chosen point. Of course the circle radius will differ in each plane in the general case: we will note it for example R_1 in the plane $(\mathbf{e}_1, \mathbf{n})$ and R_2 in the plane $(\mathbf{e}_2, \mathbf{n})$. The **mean** (or arithmetic) **curvature** κ of the surface at the considered point is

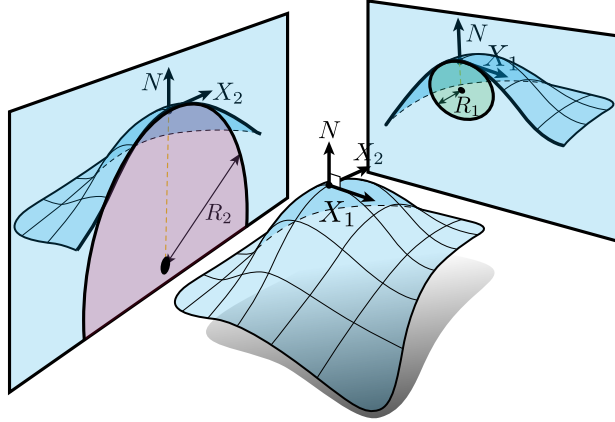


Figure 2.6: A curved surface portion intersected with a plane displays different radii of curvature depending on the plane orientation.

defined as the sum of the two circle curvatures :

$$\kappa \equiv \frac{1}{R_1} + \frac{1}{R_2}. \quad (2.28)$$

This definition calls for two remarks. The first one regards the unicity of κ 's definition. Indeed we might envisage another set of two orthogonal planes, each of them also containing \mathbf{n} (obtained via a simple rotation around \mathbf{n}). We would then get two other values for R_1 and R_2 . Remarkably, it can be shown in surface geometry that if R_1 and R_2 are not defined in an univocal way, the sum $\frac{1}{R_1} + \frac{1}{R_2}$ is independent of the planes choice! The curvature κ is a surface **invariant** (except in ill-defined cases, such as surfaces with cusps or corners – in which case the curvature diverges). The second remark is about the curvature sign. Curvature radii are signed quantities, considered positive by convention if the curvature centre is inside the surface, and negative otherwise (to differentiate what is inside from what is outside, we still use the exterior normal convention). It is therefore possible to have a surface of negative curvature.

▷ **Curvature of a sphere.** To illustrate this notion, let's consider a simple sphere of radius R . At a given point of the surface, the normal vector is given by \mathbf{e}_r and the two perpendicular

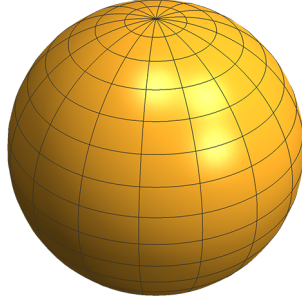


Figure 2.7: A sphere.

planes intersecting the sphere will be two (exact) circles each of radius R . As a consequence we will have:

$$\kappa_{\text{sphere}} = \frac{2}{R}. \quad (2.29)$$

▷ **Extension to general surfaces.** The previous approach, although visual and making direct contact with the meaning of curvature, suffers from some shortcomings. Indeed, beyond

elementary shapes (cylinder, cone, axisymmetric surfaces etc) it appears difficult to identify the relevant curvature radii for more general surfaces, such as the wavefield described by equation (2.24).

Fortunately there exists an alternate definition for the curvature that comes from surface differential geometry. This alternate definition allows for an easy computation of curvature in every situations:

$$\kappa \equiv \nabla_s \cdot \mathbf{n}. \quad (2.30)$$

Here the operator ∇_s represents the surface divergence. In practice we will calculate the (full) divergence of the vector field \mathbf{n} defined in every point of space, and then simply consider the restriction of this field at the interface. Now an example to shed some light over this definition.

▷ **Curvature of a sphere (again).** Let's consider again the sphere example. In order to determine \mathbf{n} , we introduce the “colour function” $\mathcal{S}(r) = r - R$. Its normalised gradient gives $\mathbf{n} = \mathbf{e}_r$ in every point of space – and in particular at the sphere' surface. The divergence of \mathbf{e}_r reads *in every point of space*:

$$\nabla \cdot \mathbf{e}_r = \frac{1}{r^2} \frac{\partial}{\partial r} (r^2 \times 1) = \frac{2}{r} \quad (2.31)$$

The restriction of this field *to the sphere' surface* gives the curvature:

$$\kappa_{\text{sphere}} = \nabla \cdot \mathbf{e}_r|_{r=R} = \frac{2}{r}|_{r=R} = \frac{2}{R}. \quad (2.32)$$

▷ **Curvature of a wavefield.** Let's go back to the wavefield equation (2.24). The divergence of the normal vector field (2.27) in each point of space is:

$$\kappa = -\frac{\Delta_{\parallel}\zeta}{\sqrt{1 + \zeta_x^2 + \zeta_y^2}} + \frac{\zeta_x(\zeta_x\zeta_{xx} + \zeta_y\zeta_{yx}) + \zeta_y(\zeta_x\zeta_{xy} + \zeta_y\zeta_{yy})}{(1 + \zeta_x^2 + \zeta_y^2)^{3/2}}, \quad (2.33)$$

where $\Delta_{\parallel} \equiv \frac{\partial^2}{\partial x^2} + \frac{\partial^2}{\partial y^2}$ represents the horizontal Laplace operator. We denote in the previous expression differentiation with indices, so that $\zeta_{yy} = \frac{\partial^2\zeta}{\partial y^2}$. We see that it would have been difficult to establish this relation with circles tangenting the surface! We finally note that in the limit of slender slope, where ζ_x, ζ_y are *a priori* much smaller than 1, the expression simplifies significantly to become

$$\kappa \simeq -\Delta_{\parallel}\zeta \quad \text{in the limit of slender slopes.} \quad (2.34)$$

Yet another manifestation of Laplace operator!

2.5 Young-Laplace's pressure jump

Having clarified the notion of surface curvature, we can go back to the estimation of the effective surface tension force exerted on a *curved* interface portion. To do so we consider the elementary surface portion described in figure 2.8. This elementary surface is subtended by two elementary arcs of curvilinear lengths $\delta\ell_1$ and $\delta\ell_2$. To first order the surface is then given by

$$\delta S = \delta\ell_1 \delta\ell_2.$$

These two elementary arcs are linked to the two curvature radii R_1 and R_2 by the infinitesimal angles $\delta\theta$ and $\delta\psi$ represented on figure 2.8 :

$$\left\{ \begin{array}{l} \delta\ell_1 = R_1 \delta\theta \\ \delta\ell_2 = R_2 \delta\psi \end{array} \right. \quad (2.35a)$$

$$(2.35b)$$

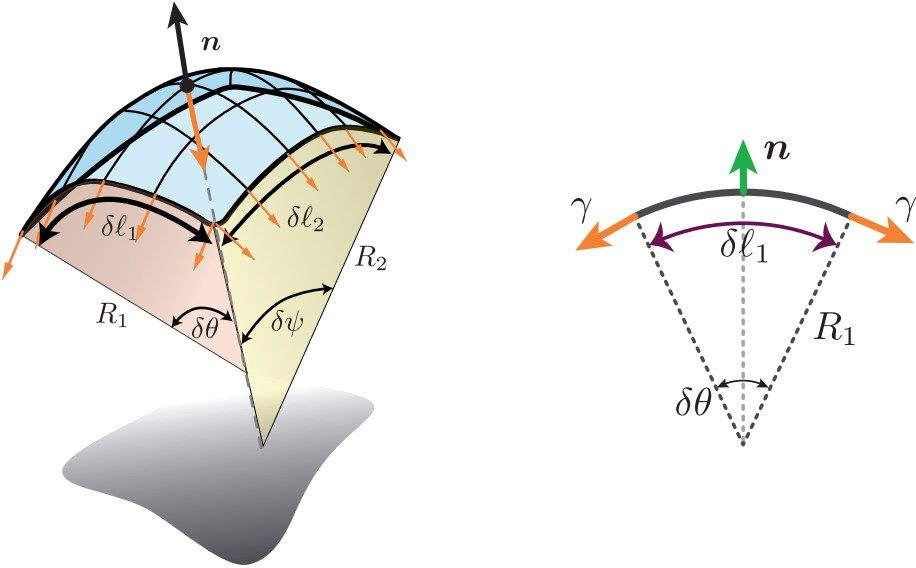


Figure 2.8: Left: a portion of curved interface is subjected to an effective force that depends both on surface tension and on geometry $-\gamma\kappa \mathbf{n} \delta S$. Right: sketch of the forces acting on a surface slice showing that contributions along the normal add up.

To quantify the action of the forces, start by considering the cut indicated on figure 2.8 (right). The two contributions of intensity γ are each inclined by $\delta\theta/2$ with respect to the tangent at the considered point. As a result, the projection along the tangent \mathbf{t} and the normal \mathbf{n} are:

$$\left\{ \begin{array}{ll} \text{projection along } \mathbf{t} : & \gamma \cos(\delta\theta/2) - \gamma \cos(\delta\theta/2) = 0 \\ \text{projection along } \mathbf{n} : & -\gamma \sin(\delta\theta/2) - \gamma \sin(\delta\theta/2) \simeq -2\gamma\delta\theta/2 = -\gamma\delta\theta \end{array} \right. \quad (2.36)$$

This is true for each cut along the path $\delta\ell_2$, so that the contribution of surface tension for these two opposite sides is $-\gamma\delta\theta\delta\ell_2$ along \mathbf{n} . We can repeat this line of reasoning for the two other sides, and we obtain the total contribution of surface tension on this small curved element:

$$\delta f_{\text{cap}} = -\gamma (\delta\theta\delta\ell_2 + \delta\psi\delta\ell_1) \mathbf{n}. \quad (2.38)$$

We can reexpress this relation with the help of the curvature radii (2.35):

$$\delta f_{\text{cap}} = -\gamma \left(\frac{1}{R_1} \delta\ell_1 \delta\ell_2 + \frac{1}{R_2} \delta\ell_1 \delta\ell_2 \right) \mathbf{n}, \quad (2.39)$$

so that finally:²⁰

$$\delta f_{\text{cap}} = -\gamma\kappa \mathbf{n} \delta S. \quad (2.44)$$

²⁰This result could have been obtained directly by application of the **surface divergence theorem** which can be stated as:

$$\oint_C \phi \mathbf{p} d\ell = \iint_S \nabla_s \phi dS - \iint_S \phi \mathbf{n} \kappa dS, \quad (2.40)$$

where S is a portion of a (curved) surface bounded by the contour C . In this expression $\nabla_s \equiv \nabla - \mathbf{n}(\mathbf{n} \cdot \nabla)$ is the *surface gradient*, and \mathbf{p} is a vector tangent to the surface but normal to the contour such that $\mathbf{p} = \mathbf{t} \times \mathbf{n}$. This formula is reminiscent of its 3D version $\iint f \mathbf{n} dS = \iiint \nabla f dV$ except for an extra term involving the curvature of the surface. Actually this extra term may be seen as rooted in a 2D extension of the Frenet-Serret formulae linking curvature, normal and rate of variation of the tangent, see also (2.47). The surface divergence theorem can be demonstrated simply with Stokes' theorem as follows. Let's start by considering a vector field \mathbf{b} defined on the surface (and not necessarily tangent to the surface – \mathbf{b} can really be any vector field). Integrating $\mathbf{b} \cdot \mathbf{p}$ on

In other words a small curved surface element will be accelerated towards its curvature centre with a force of intensity proportional to both surface tension and curvature. The force exerted on an element therefore depends on its geometry!

Let's stop for a moment and discuss the consequences of such a force. From the previous expression we might be tempted to conclude that each element of a water droplet is accelerated towards its centre, and that the droplet should collapse onto itself. To understand how droplets and other interfaces can withstand this force and remain at equilibrium, we have to remember that droplets are made of a liquid (e.g. water) that is hardly compressible. In practice this incompressibility constraint is guaranteed²¹ with the help of a pressure field that will balance the effect of surface tension. Actually, a pressure field is present in the liquid, even at equilibrium. As seen in chapter 1 the pressure force exerted onto the small considered surface element will be:

$$\delta \mathbf{f}_{\text{pressure}} = (p_{\text{int}} - p_{\text{ext}}) \mathbf{n} \delta S.$$

The interface portion equilibrium condition will then be:

$$\delta \mathbf{f}_{\text{cap}} + \delta \mathbf{f}_{\text{pressure}} = 0, \quad (2.45)$$

so that

$$\Delta p = p_{\text{int}} - p_{\text{ext}} = \gamma \kappa. \quad (2.46)$$

To ensure equilibrium, a **pressure jump** will be established across an interface. This surprising result, due to Young and Laplace, implies that a millimetric rain droplet can sustain overpressure of $\gamma \kappa \approx 7 \times 10^{-2} \times \frac{2}{10^{-3}} = 140$ Pa with respect to the atmosphere, and a micron-sized fog droplet will endure an overpressure of $\approx 7 \times 10^{-2} \times \frac{2}{10^{-6}} = 1.4 \times 10^5$ Pa, thus 1.4 bars more than atmospheric pressure!

2.5.1 Surface tension?

We followed in the previous analysis Young's viewpoint according to which the interface would be taut by a constant surface tension γ . We also recovered Laplace's result of the pressure jump

\mathcal{C} yields:

$$\begin{aligned} \oint_{\mathcal{C}} \mathbf{b} \cdot \mathbf{p} d\ell &= \oint_{\mathcal{C}} \mathbf{b} \cdot (\mathbf{t} \times \mathbf{n}) d\ell = \oint_{\mathcal{C}} (\mathbf{n} \times \mathbf{b}) \cdot \mathbf{t} d\ell \\ &= \iint_S \nabla \times (\mathbf{n} \times \mathbf{b}) \cdot \mathbf{n} dS \\ &= \iint_S (\mathbf{n} (\nabla \cdot \mathbf{b}) - \mathbf{b} (\nabla \cdot \mathbf{n}) - (\mathbf{n} \cdot \nabla) \mathbf{b} + (\mathbf{b} \cdot \nabla) \mathbf{n}) \cdot \mathbf{n} dS \end{aligned}$$

The last term here vanishes: this is best seen by writing it using Einstein convention $b_j n_i n_{i,j}$, and remarking that $n_i n_{i,j} = \frac{1}{2} (n_i n_i)_{,j} = 0$ because $n_i n_i = 1$. Now if we take $\mathbf{b} = \phi \mathbf{c}$ with \mathbf{c} an arbitrary *constant* vector, we get:

$$\mathbf{c} \cdot \left[\oint_{\mathcal{C}} \phi \mathbf{p} d\ell \right] = \mathbf{c} \cdot \left[\iint_S (\nabla \phi - \phi \mathbf{n} (\nabla \cdot \mathbf{n}) - \mathbf{n} (\mathbf{n} \cdot \nabla \phi)) dS \right]. \quad (2.41)$$

Upon remarking that for this equation to hold for any \mathbf{c} , the bracket terms have to coincide, and further noting that $\nabla \cdot \mathbf{n} \equiv \kappa$, we recover (2.40).

Finally, using this expression we see that the correct general expression for δf_{cap} is

$$\delta f_{\text{cap}} = \nabla_s \gamma \delta S - \gamma \kappa \mathbf{n} \delta S, \quad (2.42)$$

valid for any space-varying surface tension.

Note: for completeness we might also define a *surface divergence operator* such that the surface divergence of a vector \mathbf{b} is written

$$\nabla_s \cdot \mathbf{b} = [\nabla - \mathbf{n} (\mathbf{n} \cdot \nabla)] \cdot \mathbf{b} = [\nabla \times (\mathbf{n} \times \mathbf{b})] \cdot \mathbf{n} + (\mathbf{b} \cdot \mathbf{n})(\nabla \cdot \mathbf{n}). \quad (2.43)$$

With this last expression it becomes apparent that the surface divergence of \mathbf{n} is just the restriction of the full divergence of \mathbf{n} to the surface, i.e. $\nabla_s \cdot \mathbf{n} = \nabla \cdot \mathbf{n}$ on the surface.

²¹Note: even in compressible fluids (ex: bubble) a pressure field is established to counterbalance the effect of capillary force.

when traversing a curved interface. Laplace did not suppose a distributed surface tension but only attractive forces between molecules. But as we have seen in the previous part, it is possible to switch mathematically from a tangent force representation to an effective normal force, and the reverse. Our demonstration is in fact the expression of a generalisation of Frénet's formulae to three dimensions:

$$\oint_C \mathbf{p} d\ell = - \iint_A \kappa \mathbf{n} dS, \quad (2.47)$$

where \mathbf{p} is a vector tangent to the interface and C a closed curve over the interface (Tryggvason *et al.*, 2011). From this, we may wonder if surface tension exists *really*, or if it is not simply a convenient mathematical trick to describe the attractive interactions between molecules. It

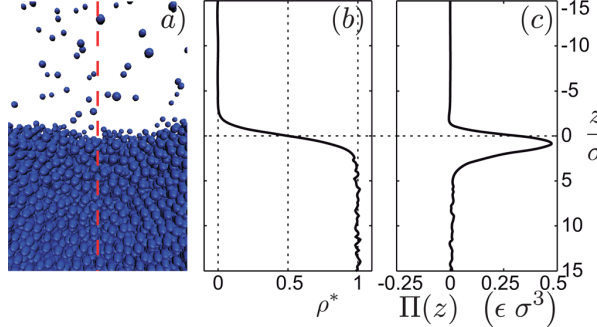


Figure 2.9: Dynamic molecular simulations show that in the vicinity of an interface, molecules are farther apart than in the liquid bulk. This depletion is associated with an increase of attractive force between molecules at the surface. The macroscopic consequence of this increase is the emergence of surface tension (Marchand *et al.*, 2011).

is now possible to use dynamic molecular simulations to answer this question. As shown in figure 2.9, there exists a force parallel to the interface that stems from a depletion in near surface molecules: surface tension has therefore a physical reality! (Berry, 1971; Marchand *et al.*, 2011).

2.5.2 Stress (dis-)continuity

With the notion of *stress*, the previous result may easily be extended to the case of moving interfaces. To do so let's consider an elementary volume in the shape of a camembert box leaning on each side of the interface, see figure 2.2. Now we let the volume thickness tend to 0, so that both the mass and the momentum of the element tend to zero as well. As a result the sum of the forces acting on this volume must be zero as well. We have already seen with (2.42) that the net sum of interfacial stresses is $\nabla \gamma \delta S - \gamma \kappa \mathbf{n} \delta S$. The stress exerted by the exterior medium is $\boldsymbol{\sigma}_{\text{ext}} \mathbf{n}_{\text{ext}} \delta S$, and similarly for the stress exerted by the interior medium $\boldsymbol{\sigma}_{\text{int}} \mathbf{n}_{\text{int}} \delta S$, with $\mathbf{n}_{\text{ext}} = -\mathbf{n}_{\text{int}} = \mathbf{n}$. The condition for interface equilibrium will thus be:

$$(\boldsymbol{\sigma}_{\text{ext}} - \boldsymbol{\sigma}_{\text{int}}) \mathbf{n} = -\nabla_s \gamma + \gamma \kappa \mathbf{n}. \quad (2.48)$$

This is a really general relation that expresses a **stress jump** at the interface. Note that in the particular static case where $\sigma_{ij} = -p \delta_{ij}$ with constant surface tension, this relation becomes:

$$\Delta p = p_{\text{int}} - p_{\text{ext}} = \gamma \kappa, \quad (2.49)$$

which is naturally the Laplace pressure jump seen in (2.46).

2.6 Equilibrium shape for a meniscus

We now have all the keys to determine interface shapes under the influence of surface tension. As an illustration we will consider in this last part the equilibrium shape for a meniscus. A meniscus

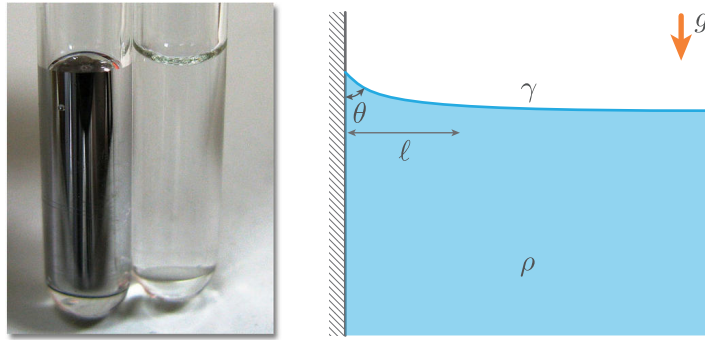


Figure 2.10: Left: mercury or water contained in test tubes exhibit sharply different menisci (Creative Commons). Right: equilibrium profile for a meniscus, parameterised by the wetting angle at the wall.

is the particular shape adopted by a liquid-gas interface near a wall (figure 2.10 left). Actually at the contact of a wall, an interface displays a *contact angle* that depends on the chemical nature of the liquid and of the wall: water or alcohol on glass or metal will have contact angles smaller than $\frac{\pi}{2}$ (*wetting* or *hydrophilic* case) whereas water on wax, on a non-stick frying pan or mercury over glass will display contact angles larger than $\frac{\pi}{2}$. The corresponding case will qualify as *non-wetting* or *hydrophobic*.

▷ **Equation for the meniscus.** At the wall contact, the interface forms an angle θ . Yet far from the wall the interface is back to planar under the influence of gravity. In between, the interface will adopt a shape of a membrane “taut” by the action of surface tension – and under the influence of gravity. Over which lengthscale ℓ does this matching take place? We can give a first estimation with dimensional analysis. Here $\ell = f(\rho, \gamma, g)$, and as $[\gamma] = \text{MT}^{-2}$ a direct application of π theorem informs us that this matching length will be proportional to:

$$\ell_{\text{gc}} = \sqrt{\frac{\gamma}{\rho g}}. \quad (2.50)$$

This is the *gravity-capillary length* (sometimes simply coined capillary length).

Let's now determine the equation driving the shape for the interface. To this end, let's introduce first the z coordinate whose origin will be at the interface height very far from the wall. We will monitor the interface height at each point with the function $z = h(x)$. At the interface level the pressure jump relation (2.46) allows us to write:

$$p(z = h) - P_{\text{atm}} = \gamma \kappa, \quad (2.51)$$

where $p(z = h)$ is the pressure in the liquid near the interface, and P_{atm} is the atmospheric pressure. Before going further, let's remark that the interface curvature centre is *outside* (of the liquid): the pressure jump will therefore be negative, which implies that the liquid pressure will be *lower* than atmospheric pressure.

In the liquid, hydrostatics applies, so $p(z) = P_{\text{atm}} - \rho g z$. We therefore have:

$$-\rho g h = \gamma \kappa, \quad (2.52)$$

or

$$h = -\ell_{\text{gc}}^2 \kappa. \quad (2.53)$$

This is the interface equation.

▷ **Equilibrium profile in the slender slope limit.** In general this equation is quite difficult to solve because of its nonlinearities. Indeed, the interface curvature reads:

$$\kappa(x) = -\frac{h''}{(1+h'^2)^{3/2}}. \quad (2.54)$$

But in the slender slope limit, corresponding to contact angles close to $\frac{\pi}{2}$ – and anyway always true sufficiently far from the wall –, $h' \ll 1$ and $\kappa \simeq -h''$. As a result (2.53) admits exponential solutions of the type $e^{x/\ell_{\text{gc}}}$ and $e^{-x/\ell_{\text{gc}}}$. Only the latter solution allows to recover a flat profile at infinity. In the slender slope limit, the interface is therefore described with:

$$h(x) = Ae^{-x/\ell_{\text{gc}}}, \quad (2.55)$$

where A is a constant set by the boundary conditions. In the slender slope limit, we will have near the wall $h' = -(\frac{\pi}{2} - \theta)$, so:

$$h(x) = \ell_{\text{gc}}(\frac{\pi}{2} - \theta)e^{-x/\ell_{\text{gc}}}. \quad (2.56)$$

▷ **Meniscus weight.** If we were to suppress the wall in figure 2.10 right, the interface would naturally get back to the position $z = 0$. A question is therefore: what bears the meniscus weight? (because it is not the liquid pressure far below). The only remaining candidate is the wall: the wall exerts a force of intensity γ parallel to the interface and therefore lifts the liquid. In vertical projection, this force has a contribution $F_{\text{cap}} = \gamma \cos \theta$, which has to balance the meniscus weight.

We can verify this fact by calculus with the help of equation (2.53). Let's introduce the angle ϕ that the interface forms locally with the horizontal ($\phi = \theta - \pi/2$). Whenever we follow an elementary interface portion ds , this angle changes by an amount $d\phi$ such that $ds = R d\phi = -\frac{1}{\kappa} d\phi$. From this relation we deduce $\kappa = -\frac{d\phi}{ds}$. The equation for the meniscus then becomes:

$$-\rho g h(s) = -\gamma \frac{d\phi}{ds}. \quad (2.57)$$

On remarking that $\cos \phi = \frac{dx}{ds}$, we see that the meniscus weight can be written as:

$$P = -\rho g \int_0^\infty h(x) dx = -\rho g \int_0^\infty h(s) \cos \phi ds. \quad (2.58)$$

Thus, by multiplying the interface equation by $\cos \phi$ we get:

$$\underbrace{-\rho g \int_0^\infty h(s) \cos \phi ds}_P = -\gamma \int_0^\infty \cos \phi \frac{d\phi}{ds} ds = -\gamma [\sin \phi]_0^\infty = \gamma \sin \phi_0 = \underbrace{-\gamma \cos \theta}_{-F_{\text{cap}}}. \quad (2.59)$$

Chapter 3

Viscous flows

Whenever the viscous diffusion timescale $\rho L^2/\mu$ is short with respect to inertial L/U or imposed ω^{-1} timescales, flows will be dominated by viscosity. This situation occurs of course if the viscosity of the material is high, e.g. with mud, magma or glass melt (figure 3.1) but not only. Glaciers were reported to flow as early as 1873 (Aitken, 1873). These so-called *rivers of ice* indeed flow, albeit very slowly – typically less than a metre a day – making inertial phenomena irrelevant (figure 3.1; see also the slow motion footage taken by BBC Earth Lab <https://youtu.be/ghC-UtOfW4o>). At very small scales where bacteria and algae evolve, diffusion competes and usually overcomes inertial effects. As a result, microorganisms living at such scales have evolved non-intuitive strategies to move as we will see next.

In all these examples the ratio between the diffusive and inertial timescales – the Reynolds number $\text{Re} = \rho UL/\mu$ – is much smaller than one. Fluid motion can still be described with the Navier-Stokes equations in this context, but we will now see that the condition $\text{Re} \ll 1$ implies that some terms have not the same order of magnitude than others. Exploiting the low-Re number hypothesis will enable us to obtain the relevant equation for viscous flow motion, the **Stokes equation**.

3.1 Low-Re number flows

Whenever fluids have a high viscosity μ , or flow at small scale L or with a low velocity U , the equations describing their motion can be greatly simplified. This can be seen by non dimensionalising the equations of motions with the natural scales of the problem $\mathbf{U} = U\mathbf{u}$, $\mathbf{X} = L\mathbf{x}$ (here we denote dimensioned quantities with capital letters). The pressure can be made dimensionless with a natural viscous scale $P = \mu \frac{U}{L} p$ and finally if there is a imposed timescale ω^{-1} (e.g. the inverse of the swimming frequency) we may write $T = \omega^{-1} t$.

$$\text{Re}_\omega \frac{\partial \mathbf{u}}{\partial t} + \text{Re} (\mathbf{u} \cdot \nabla) \mathbf{u} = -\nabla p + \Delta \mathbf{u}. \quad (3.1)$$

Here, two Reynolds numbers appear:

$$\text{Re}_\omega = \frac{\rho L^2 \omega}{\mu} \quad \text{and} \quad \text{Re} = \frac{\rho U L}{\mu}, \quad (3.2)$$

which each may be interpreted as a ratio of timescales as seen in the introduction of this chapter. Note that for e.g. flagellae propelled microorganisms, the oscillatory Reynolds number Re_ω involves the relevant velocity scale $L\omega$ for the fluid set into motion by the oscillating flagella. In equation (3.1) each variable has been rescaled with its expected range of variation range. Therefore each of the force terms (right hand side) is $\mathcal{O}(1)$ while the unsteady and convective part of momentum variation (left hand side) are respectively of order Re_ω and Re . For flows

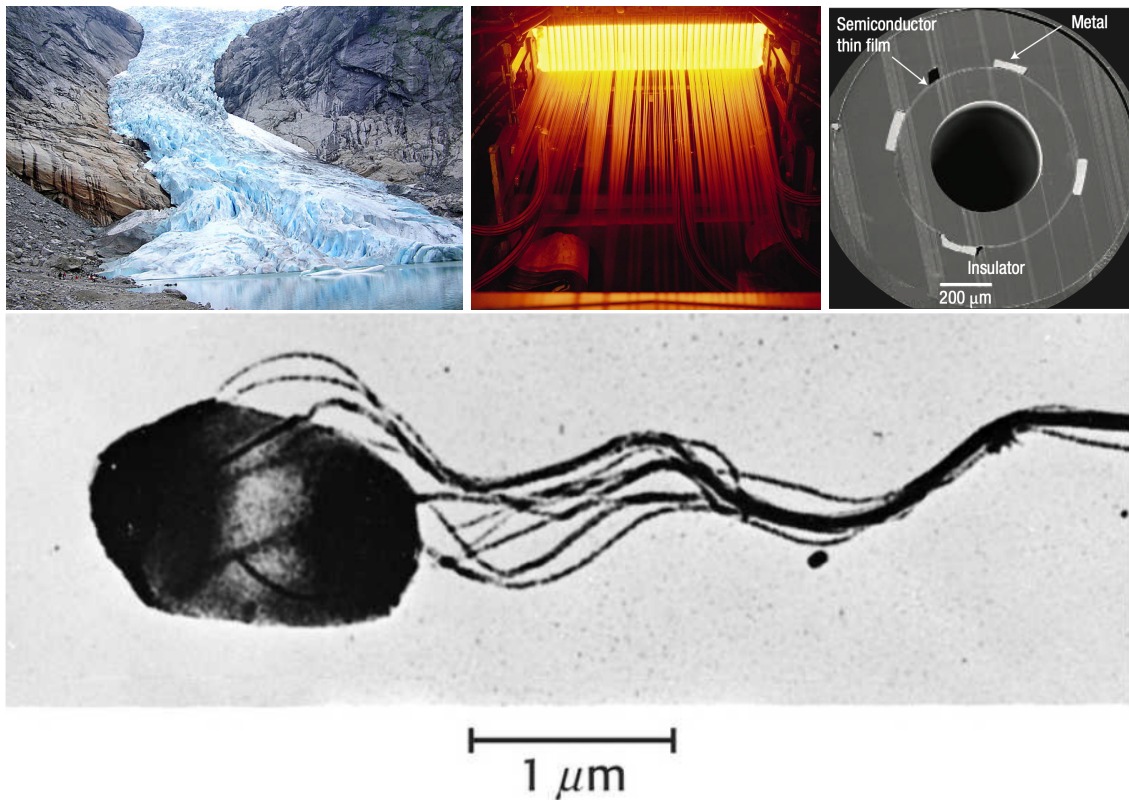


Figure 3.1: **Flows dominated by viscosity.** Top left : the Briksdalsbreen glacier in Norway is slowly flowing into a lake (photograph by vicrogo, public domain). Top middle: glass fibre manufacturing (photograph Saint-Gobain). Top right: modern optical fibre drawing process allow to produce multilayered fibres ([Abouraddy et al., 2007](#)). Bottom: micron-sized salmonellae swim with the help of a bundle of rotating helicoidal flagellae ([Elgeti et al., 2015](#)).

Organism	length	velocity	frequency	Re	Re_ω
Bacterium	10 μm	10 $\mu\text{m}/\text{s}$	100 Hz	10^{-4}	10^{-2}
Spermatozoon	100 μm	100 $\mu\text{m}/\text{s}$	10 Hz	10^{-2}	10^{-1}
Ciliate	100 μm	1 mm/s	10 Hz	10^{-1}	10^{-1}
Tadpole	1 cm	10 cm/s	10 Hz	10^3	10^3
Small fish	10 cm	10 cm/s	10 Hz	10^4	10^5
Penguin	1 m	1 m/s	1 Hz	10^6	10^6
Sperm whale	10 m	1 m/s	0.1 Hz	10^7	10^7

Table 3.1: **Reynolds number for different living organisms.** Bacteria, spermatozoa and ciliates are all characterised by Reynolds numbers Re and Re_ω much smaller than unity. The flowing fluid in their vicinity is therefore accurately described with the Stokes equation. Data from Lauga (2020).

without an imposed frequency (flowing glass melts or glacier flow), these two numbers will be identical. But if the flow is produced by an oscillating object, they can significantly differ. Table 3.1 reports an estimation of these two Reynolds numbers for a range of organisms living in aqueous environments, where it can be seen that the double condition $\text{Re}_\omega \ll 1$, $\text{Re} \ll 1$ is fulfilled in the realm of microorganisms.

In this limit, the Navier-Stokes equation reduces to the much simpler **Stokes equation**:

$$\nabla p = \Delta \mathbf{u} \quad \text{or, in its dimensioned version: } \nabla P = \mu \Delta \mathbf{U}. \quad (3.3)$$

▷ **Cauchy equation.** The Stokes equation may also be rewritten as the following *Cauchy equation*:

$$\nabla \cdot \boldsymbol{\sigma} = 0. \quad (3.4)$$

With this formulation it becomes apparent that viscous flows are *force free*: in absence of significant inertia, the forces balance each other.

3.2 Stokes flow's properties

▷ **Linearity.** The Stokes equation (3.3) is **linear**: this means that elementary solutions can be used to construct more involved ones, either as a weighted sum of individual singular solutions or as a convolution integral between an appropriate Green's function and data boundaries. For example, the knowledge of the velocity \mathbf{U} at the boundary S of a fluid domain allows to express the fluid velocity \mathbf{u} at any point \mathbf{r} of the domain as:

$$u_i(\mathbf{r}) = \int_S g_{ij}(\mathbf{r}|\mathbf{r}_0) U_j(\mathbf{r}_0) dS(\mathbf{r}_0). \quad (3.5)$$

Similarly a knowledge of the *forces*²² \mathbf{F} at the domain boundary would lead to the following formal form for the solution:

$$u_i(\mathbf{r}) = \int_S g_{ij}(\mathbf{r}|\mathbf{r}_0) F_j(\mathbf{r}_0) dS(\mathbf{r}_0). \quad (3.6)$$

A practical consequence of these relations is the **uniqueness** of the Stokes flow solution: the boundary conditions uniquely determine the solution. This contrasts with the multitude of solutions that can be encountered for higher Reynolds number and originate (mathematically) from the nonlinear term of the Navier-Stokes equation.

²²Mixed boundary conditions, constituted of velocity data on part of the boundaries, and forces data on other, can be treated with the same procedure.

▷ **Reversibility.** Another quite surprising property of Stokes flow is their **reversibility**. This



Figure 3.2: **Stokes flow kinematic reversibility.** Left: a drop of dye is injected in a quiescent viscous liquid filling the space between two concentric cylinders. Middle: on rotating the inner cylinder with a handle, the dye is stretched and stirred so that it becomes barely visible. Right: reversing the cylinder motion allows to relocate the dye's drop at its initial position almost perfectly (from G.I. Taylor's *Low-Reynolds-Numbers Flows* movie © National Committee for Fluid Mechanics Films / Education Development Center).

counter-intuitive phenomenon is illustrated on figure 3.2. A drop of dye mixed by differential rotation in a Taylor-Couette apparatus can be “unmixed” by reversing the boundary velocity. From a mathematical point of view, this reversal property can be understood by noting that changing the sign of the boundary velocity in (3.5) simply changes the sign of the solution. Alternatively it can also be noted that the transformation $(\mathbf{u}, p) \rightarrow (-\mathbf{u}, -p)$ also yields a solution of the Stokes equation (3.3) (provided that the boundary conditions are transformed as well).

▷ **A paradox?** From a physical point of view, this reversibility is more troublesome: if diffusion is associated with irreversible microscopic phenomena, how can diffusion-dominated flows be reversible? Actually the reversal illustrated figure 3.2 is purely *kinematic*: while the velocity fields have been reversed and the drop of dye retrieved its overall initial position, molecular diffusion has acted on the microscopic scale as evidenced by the slightly smeared aspect of the final drop, heat has been produced by viscous dissipation and the entropy of the final state is indeed higher than that of the starting state.

3.3 Moving in a viscous world

A paradigm for motion in viscous fluids is the settlement of a sphere, first investigated by Stokes. Arguably lengthy calculations (see tutorial) allow to obtain the expression for the velocity and pressure field around a sphere of radius R settling steadily at velocity $-\mathbf{V}^\infty$ in a quiescent viscous fluid in its reference frame:

$$\begin{cases} u_i = -\frac{3R}{4} V_j^\infty \left(\frac{\delta_{ij}}{r} + \frac{r_i r_j}{r^3} \right) - \frac{3R^3}{4} V_j^\infty \left(\frac{\delta_{ij}}{3r^3} - \frac{r_i r_j}{r^5} \right), \\ p - p_\infty = -\frac{3\mu R}{2} \frac{V_j^\infty r_j}{r^3}. \end{cases} \quad (3.7a)$$

$$(3.7b)$$

These expressions allow to evaluate the stresses at the sphere surface and to deduce the well-known **Stokes drag** $\mathbf{F} = 6\pi\mu R \mathbf{V}^\infty$ exerted on the sphere.

An alternative and very useful viewpoint is to present these results in terms of the force $\mathbf{f} = -\mathbf{F}$ exerted by the sphere on the fluid:

$$u_i = \underbrace{\frac{1}{8\pi\mu} f_j \left(\frac{\delta_{ij}}{r} + \frac{r_i r_j}{r^3} \right)}_{\text{Stokeslet contribution}} + \frac{R^2}{8\pi\mu} f_j \left(\frac{\delta_{ij}}{3r^3} - \frac{r_i r_j}{r^5} \right). \quad (3.8)$$

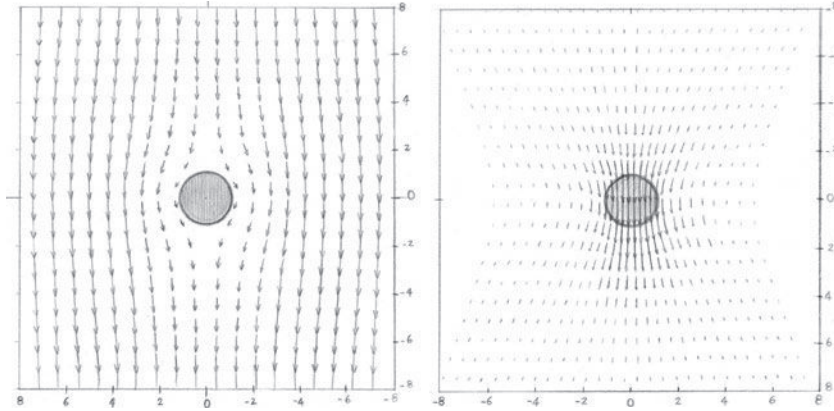


Figure 3.3: Spheres in viscous flows. Left: A fixed sphere deflects the surrounding flowing fluid. Right: A moving sphere in a still environment pushes the fluid in its vicinity (Guazzelli & Morris, 2011).

Interestingly if we were to shrink the size of the sphere to 0 while keeping the force constant, the only remaining term in the flow field would be the first one. This so-called Stokeslet contribution is of fundamental importance in suspension dynamics, bacteria hydrodynamics and more generally in the modelling of viscous flows.

3.3.1 Point force induced flow: the Stokeslet

The Stokeslet is a fundamental solution for the Stokes equation, and describes the flow that would be induced by a point force $\mathbf{f}\delta(\mathbf{x} - \mathbf{x}_0)$ located at $\mathbf{x} = \mathbf{x}_0$. The corresponding velocity and pressure fields therefore satisfy the following *forced Stokes equation*:

$$-\nabla p + \mu\Delta\mathbf{u} + \mathbf{f}\delta(\mathbf{x} - \mathbf{x}_0) = 0. \quad (3.9)$$

Note that in this expression \mathbf{f} is a constant vector.

The flow field solution is termed **Stokeslet** and is characterized by:

$$\mathbf{u}_{\text{stokeslet}}|_i(\mathbf{x}) = \frac{1}{8\pi\mu} \mathcal{S}_{ij}(\mathbf{x}|\mathbf{x}_0) f_j, \quad (3.10)$$

with \mathcal{S}_{ij} being the *Oseen-Burgers tensor* defined as:

$$\mathcal{S}_{ij} = \frac{\delta_{ij}}{r} + \frac{r_i r_j}{r^3}. \quad (3.11)$$

Let's now see in more details how this solution is constructed. To do so it will prove useful to first introduce the Green's function for Laplace equation $g(\mathbf{x}|\mathbf{y})$.

▷ **Green's function for Laplace equation.** The Green's function $g(x|y)$ for Laplace equation is the function satisfying:

$$\Delta g(\mathbf{x}|\mathbf{y}) = \delta(\mathbf{x} - \mathbf{y}). \quad (3.12)$$

It is an harmonic function of space except at the point $\mathbf{x} = \mathbf{y}$ where it is singular. Symmetry considerations on this function suggest that it only depends on the radius $r = \|\mathbf{x} - \mathbf{y}\|$. On integrating over a small ball containing the singularity we get:

$$\oint \frac{\partial g}{\partial r} dS = 1,$$

so that the Green's function for Laplace equation is:

$$g(\mathbf{x}|\mathbf{y}) = -\frac{1}{4\pi r}. \quad (3.13)$$

▷ **Stokeslet obtention.** With the help of the Green's function for Laplace equation, the divergence of the forced Stokes equation (3.9) may be written as

$$\Delta \left(p - \mathbf{f} \cdot \nabla \left(-\frac{1}{4\pi r} \right) \right) = 0. \quad (3.14)$$

The maximum principle for harmonic functions allows us to directly write the pressure as:

$$p = \mathbf{f} \cdot \nabla \left(-\frac{1}{4\pi r} \right). \quad (3.15)$$

Injecting this form for the pressure in equation (3.9) we obtain:

$$\mu \Delta u_i = \frac{1}{4\pi} \left(\underbrace{\delta_{ij} \frac{\partial}{\partial x_k} \frac{\partial}{\partial x_k}}_{I\Delta} \left(\frac{1}{r} \right) - \underbrace{\frac{\partial}{\partial x_i} \frac{\partial}{\partial x_j}}_{\nabla\nabla} \left(\frac{1}{r} \right) \right) f_j. \quad (3.16)$$

From the structure of this relationship, the adventurous reader might tempt to look for a solution of the form:

$$u_i = \frac{1}{4\pi} \left(\delta_{ij} \Delta \mathcal{H} - \frac{\partial^2 \mathcal{H}}{\partial x_i \partial x_j} \right) f_j. \quad (3.17)$$

Note that this velocity field is solenoidal, as:

$$u_{i,i} = \frac{1}{4\pi} (\Delta \mathcal{H}_{,j} - \Delta \mathcal{H}_{,j}) f_j \equiv 0. \quad (3.18)$$

Injecting (3.17) into (3.16) we get:

$$\frac{1}{4\pi} (I\Delta - \nabla\nabla) \left(\mu \Delta \mathcal{H} - \left(\frac{1}{r} \right) \right) = 0. \quad (3.19)$$

This reduces to the following Poisson equation for \mathcal{H} ²³:

$$\mu \Delta \mathcal{H} = \frac{1}{r} \quad \text{with solution: } \mathcal{H} = \frac{1}{2\mu} r. \quad (3.20)$$

Noting that $r = (r_k r_k)^{1/2}$, we deduce:

$$r_{,i} = \frac{r_{k,i} r_k}{(r_m r_m)^{1/2}} \equiv \frac{x_i}{r} \quad \text{and similarly} \quad r_{,ij} = \frac{\delta_{ij}}{r} - \frac{r_i r_j}{r^3}, \quad (3.21)$$

to finally obtain the expression of the Stokeslet velocity field (3.10) we were looking for:

$$\mathbf{u}_{\text{stokeslet}} = \frac{1}{8\pi\mu} \mathbf{S}\mathbf{f}. \quad (3.22)$$

3.3.2 The motion of slender objects

We have seen that in the limit of radius shrinking down to zero, a sphere applying a force to a viscous fluid generates a Stokeslet flow. But looking back at the full expression for the flow set into motion by a sphere of finite size (3.8), it is apparent that the total contribution is actually composed of two parts: a Stokeslet and higher-order singularity – a dipole. Without entering into the details of the derivation, Hancock (1953) and Lighthill (1975) proposed to describe the fluid flows around more general, and slender, objects, as integrals of Stokeslets and

²³Note that we did not consider the integration constants because they would not appear in the velocity field expression anyway.

dipole contribution. More precisely it appears that the force exerted by a viscous fluid on a very long cylinder of radius R and length L depends on the orientation of the flow. If the flow is perpendicular to the filament axis, the force exerted on the cylinder per unit length is:

$$f_{\perp} \simeq c_{\perp} u_{\perp} \quad \text{with} \quad c_{\perp} = \frac{4\pi\mu}{\ln(L/R)}. \quad (3.23a)$$

And similarly, if the flow is now parallel to the fibre:

$$f_{\parallel} \simeq c_{\parallel} u_{\parallel} \quad \text{with} \quad c_{\parallel} = \frac{2\pi\mu}{\ln(L/R)}. \quad (3.23b)$$

Note that there is a factor 2 between f_{\perp} and f_{\parallel} . This drag anisotropy has consequences on the settling of slender objects that we shall not detail here, but the interested reader will find detailed and useful accounts in Duprat & Stone (2016) or Lauga (2020) for example.

Chapter 4

Thin viscous films

Just as slender solid structures (threads, wires, shells or plates) can be described with a set of simple equations rather than relying on full 3D elasticity, fluid flows with high aspect ratios (lacrymal film on the eye, paint coat, ink jet, atmosphere) may be depicted with equations much more simple than the Navier-Stokes equations. In this chapter, we set out to investigate the dynamics of a thin liquid film dominated by viscous effects and derive the so-called **lubrication equations** for the film.

4.1 A rippled paint coat

To contextualise and motivate our study, let's aim to depict and predict the relaxation time taken for a rippled paint coat to return to its flat equilibrium. The (aqueous) paint is to first order considered a viscous liquid ($\mu = 0.1 \text{ Pa}\cdot\text{s}$) of density $\rho = 1000 \text{ kg}\cdot\text{m}^{-3}$ and presenting a surface tension $\gamma = 50 \text{ mN}\cdot\text{m}^{-1}$ with air. The paint coat of typical height $H = 10 \mu\text{m}$ presents a characteristic rippling of wavelength $\lambda = 500 \mu\text{m}$. Preliminary experiments furthermore point out to a relaxation time of the order of 1 s (maybe a bit less). We now wish to understand both qualitatively and quantitatively this timescale, as well as to identify the scaling laws behind it.

4.2 Power & limits of dimensional analysis

We have witnessed so far that dimensional analysis is a powerful tool to obtain rapid estimates on quantities of interest. Let's conduct such an analysis here. The relaxation timescale τ is a priori a function of the aforementioned parameters, and, possibly, gravity:

$$\tau = f(\gamma, \mu, \rho, H, \lambda, g). \quad (4.1)$$

In this expression there are $k = 3$ independent dimensions, so taking ρ , γ and H as characteristic scales we get:

$$\tau = \sqrt{\frac{\rho H^3}{\gamma}} F(\varepsilon, \text{Oh}, \text{Bo}), \quad (4.2)$$

with $\varepsilon = H/\lambda$ is the aspect ratio of the liquid film (transverse lengthscale over horizontal lengthscales), $\text{Oh} = \mu/\sqrt{\rho\gamma H}$ is the Ohnesorge number (or nondimensional viscosity) and $\text{Bo} = \rho g H^2/\gamma$ is the Bond number (or nondimensional gravity). We could have started differently, supposing for example that gravity is not relevant in this problem, but in either case, dimensional analysis will always feature a unknown dependency to ε , the nondimensional ratio between lengthscales, making it difficult to conclude on pure dimensional grounds. It is a fundamental limitation of dimensional analysis for slender flows, which calls for a deeper look at the physics at play in this problem.

4.3 Quick physical analysis and order of magnitude estimate

A rippled liquid film displays alternate peaks and troughs. This geometric alternance of positive and negative curvatures reflects into a dynamic alternance of higher and lower pressure zones. Let's remark that the pressure force in the fluid $-\nabla P$ will be directed from the peaks to the troughs, hence providing a driving physical mechanism for relaxation. We can estimate rapidly the magnitude of these pressure shifts by looking at the characteristic curvature scale. The slope of the interface is (at worst) of order H/λ (if the amplitude of the disturbance a is significantly lower than H , it would rather be a/λ but let's consider the worst case where $a \sim H$). The characteristic scale for curvature is then H/λ^2 and the magnitude of the pressure difference between the ambient atmosphere and the liquid film follows:

$$p_{\text{cap}} = \gamma \kappa \sim \gamma \frac{H}{\lambda^2}. \quad (4.3)$$

The pressure gradient corresponding to this pressure distribution ensues:

$$-\nabla p_{\text{cap}} \sim -\gamma \frac{H}{\lambda^3}. \quad (4.4)$$

▷ **What about gravity?** We could have as well estimated the pressure in the liquid film considering hydrostatic pressure. Here again the peak region of the liquid film corresponds to a higher pressure area than the through region, leading to relaxation. A quick estimate of the film pressure now yields:

$$p_{\text{grav}} \sim \rho g H. \quad (4.5)$$

The gravity pressure gradient is therefore:

$$-\nabla p_{\text{grav}} \sim -\rho g \frac{H}{\lambda}. \quad (4.6)$$

In the experiment we are considering, which of capillary and gravity effects is dominant? To answer this question, let's look at the ratio between the pressure gradients:

$$\frac{\gamma H / \lambda^3}{\rho g H / \lambda} \quad \left(= \frac{\varepsilon^2}{\text{Bo}} \right). \quad (4.7)$$

With the characteristic scales given in introduction for the paint coat, this ratio is about 20, indicating that at least in this configuration gravity can safely be disregarded to first approximation.

From momentum balance analysis, the capillary driving force will either be resisted by fluid inertia, or viscous stresses, or both. Here the (thin) film is made of a viscous fluid; this suggests that pressure forces are balanced by viscosity. Let's start with this hypothesis: the capillary pressure gradient induces a flow within the film which is resisted by viscous stresses, i.e. **the flow within the liquid film is of capillary-viscous nature**:

$$\frac{\gamma H}{\lambda^3} \sim \mu \frac{U}{H^2} \quad \text{so that} \quad \underbrace{\frac{\mu U}{\gamma}_{\text{Ca}} \sim \underbrace{\left(\frac{H}{\lambda}\right)^3}_{\varepsilon^3}}. \quad (4.8)$$

From this last expression we see that requiring a balance between capillary and viscous effects imposes that the **capillary number** $\text{Ca} = \mu U / \gamma$ (measuring the relative importance of the velocity with respect to the natural capillary-viscous velocity scale γ/μ) should scale as the aspect ratio ε to the third power.

This balance allows us to estimate the (horizontal) velocity scale at which the fluid goes from the peaks to the troughs:

$$U \sim \frac{\gamma}{\mu} \left(\frac{H}{\lambda} \right)^3. \quad (4.9)$$

The rushing fluid from the neighbouring liquid crests will fill up the troughs. From (incompressible²⁴) mass conservation we can estimate the vertical component of velocity V there:

$$\frac{U}{\lambda} \sim \frac{V}{H} \quad \text{and} \quad V \sim \frac{\gamma}{\mu} \left(\frac{H}{\lambda} \right)^4. \quad (4.10)$$

This vertical velocity component is associated with a levelling up of the interface at the rate:

$$\frac{H}{\tau} \sim V, \quad (4.11)$$

where τ is the healing time for the interface, which is therefore of order:

$$\tau \sim \frac{\mu \lambda^4}{\gamma H^3}. \quad (4.12)$$

This results calls for several remarks. First we notice that more viscous liquids take longer to relax, consistently with the balance written earlier between the capillary driving force and the viscous braking. Second, this relaxation time is indeed of the form (4.2), with:

$$F(x, y, z) = \alpha \frac{y}{x^4}, \quad (4.13)$$

with α being a nondimensional prefactor. This particular scaling is impossible to find on dimensional grounds alone. Finally, we may now estimate the relaxation time taking a prefactor $\alpha \sim O(1)$, and we get $\tau \sim 100$ s, which is about two orders of magnitude higher than what is observed in experiments...

Either the physical analysis is missing a key ingredient, either the prefactor is not of order 1. To shed further light, we set out to derive the value of the prefactor by conducting a detailed asymptotic analysis of the rippled film relaxation.

4.4 Detailed asymptotic analysis: thin film flow

The physical picture just derived will guide us as a beacon to derive a more in-depth analysis of the problem. To make progress we start by nondimensionalising the problem making use of the known H and λ and the unknown U , V and δP characteristic scales:

$$\begin{cases} h = H \bar{h}, \\ x = \lambda \bar{x}, \end{cases} \quad (4.14a)$$

$$\begin{cases} y = H \bar{y}, \\ u = U \bar{u}, \end{cases} \quad (4.14b)$$

$$\begin{cases} v = V \bar{v}, \\ p = P_{\text{atm}} + \delta P \bar{p}. \end{cases} \quad (4.14c)$$

$$\begin{cases} v = V \bar{v}, \\ p = P_{\text{atm}} + \delta P \bar{p}. \end{cases} \quad (4.14d)$$

$$\begin{cases} v = V \bar{v}, \\ p = P_{\text{atm}} + \delta P \bar{p}. \end{cases} \quad (4.14e)$$

$$\begin{cases} v = V \bar{v}, \\ p = P_{\text{atm}} + \delta P \bar{p}. \end{cases} \quad (4.14f)$$

²⁴Using this type of quick physical analysis makes it easy to discuss the relevance of the incompressibility condition. Considering an incompressible evolution is justified as long as $\delta\rho/\rho \ll 1$. The density fluctuation $\delta\rho$ is connected to the pressure fluctuation δP via $\delta\rho = \delta P (\partial p / \partial \rho)^{-1}$, with $(\partial p / \partial \rho) \equiv c^2$, i.e. the speed of sound squared. For lubrication films, the pressure scale δP follows from horizontal momentum balance: $\delta P \sim \varepsilon^{-1} \mu U / H$. This means that compressible effects are not relevant as long as $U \ll \varepsilon \rho c^2 H / \mu$ or, equivalently, $\text{Ma} \ll (\varepsilon \text{Re})^{1/2}$ (here Ma stands for the Mach number). Micronic liquid films made of very viscous fluids – say one million times more viscous than water – will therefore see significant compressible effects arise as soon as the imposed velocity is of $O(\text{cm/s})$! Conversely, the liquid films freely evolving under surface tension alone under investigation here can safely be viewed as incompressible as long as $\varepsilon^2 \gamma / \rho c^2 H \ll 1$. Using the parameters given for the liquid film, $\varepsilon^2 \gamma / \rho c^2 H \sim 10^{-9}$, indeed totally justifying the incompressibility assumption.

It is important to stress that the used characteristic scales are expected **scales of variation**, meaning that all the barred quantities have no dimension and are further of order 1. The identification of the unknown scales will proceed from the expression of the first principles.

4.4.1 Preliminary: mass conservation

Before entering into the asymptotic analysis of the fluid motion, it is worth remarking that the two components of velocity are linked kinematically by mass conservation, which reads for this incompressible evolution:

$$\frac{U}{\lambda} \bar{u}_{\bar{x}} + \frac{V}{H} \bar{v}_{\bar{y}} = 0. \quad (4.15)$$

A distinguished scaling immediately reveals that $U/\lambda \sim V/H$ so that we can set

$$V = \varepsilon U, \quad (4.16)$$

and mass conservation is written:

$$\bar{u}_{\bar{x}} + \bar{v}_{\bar{y}} = 0. \quad (4.17)$$

4.4.2 Stress condition at the interface

▷ **Normal stress jump.** The starting point of the analysis is to identify the scale of pressure, as it is the driver of the flow. Pressure is set via the dynamic boundary condition (2.48) projected along the normal:

$$\mathbf{n} \cdot (\boldsymbol{\sigma}_{\text{ext}} - \boldsymbol{\sigma}_{\text{int}}) \cdot \mathbf{n} = \gamma \kappa \quad \text{at} \quad y = h. \quad (4.18)$$

This equation features geometric quantities such as the normal vector and the interface curvature κ . These can be obtained taking the following color function $\mathcal{S}(x, y, t) = y - h(x, t)$ to describe the interface:

$$\mathbf{n} = \frac{1}{\sqrt{1 + h_x^2}} \begin{pmatrix} -h_x \\ 1 \end{pmatrix} \quad ; \quad \mathbf{t} = \frac{1}{\sqrt{1 + h_x^2}} \begin{pmatrix} 1 \\ h_x \end{pmatrix} \quad ; \quad \kappa = -\frac{h_{xx}}{(1 + h_x^2)^{3/2}}. \quad (4.19)$$

Here subscripts denote differentiation, and \mathbf{t} refers to as the tangent vector to the interface. Considering the liquid in the film to be Newtonian and the evolution incompressible, we can rewrite (4.18) as:

$$-\frac{1}{\sqrt{1 + h_x^2}} \left(-(p - P_{\text{atm}})(1 + h_x^2) + 2\mu u_x h_x^2 - 2\mu (u_y + v_x) h_x + \underbrace{2\mu v_y}_{-2\mu u_x} \right) = -\gamma \frac{h_{xx}}{(1 + h_x^2)^{3/2}}. \quad (4.20)$$

This equation can be rewritten with the help of the previously introduced nondimensional quantities. Noting that $h_x = \varepsilon \bar{h}_{\bar{x}}$ we have:

$$-\delta P \bar{p} (1 + \varepsilon^2 \bar{h}_{\bar{x}}^2) - 2\mu (1 - \varepsilon^2 \bar{h}_{\bar{x}}^2) \frac{U}{\lambda} \bar{u}_{\bar{x}} - 2\mu \varepsilon h_{\bar{x}} \left(\frac{U}{H} \bar{u}_{\bar{y}} + \frac{V}{\lambda} \bar{v}_{\bar{x}} \right) = \gamma \frac{H}{\lambda^2} \frac{\bar{h}_{\bar{x}\bar{x}}}{(1 + \varepsilon^2 \bar{h}_{\bar{x}}^2)^{1/2}}. \quad (4.21)$$

Here we have crossed out quantities negligible at leading order. Rearranging, we get:

$$\boxed{-\delta P \bar{p} - 2\mu \frac{U}{\lambda} \bar{u}_{\bar{x}} - 2\mu \frac{U}{\lambda} h_{\bar{x}} \bar{u}_{\bar{y}}} = \gamma \frac{H}{\lambda^2} \bar{h}_{\bar{x}\bar{x}} \quad \text{at} \quad \bar{y} = \bar{h}. \quad (4.22)$$

It is important to remark that in this expression, the pressure contribution is of order δP , the viscous normal stress is $O(\mu U / \lambda)$ and the capillary term $O(\gamma H / \lambda^2)$. To be consistent with our initial picture, we **want** to balance the highlighted pressure and capillary terms, so we **set** the pressure scale as:

$$\delta P = \gamma \frac{H}{\lambda^2}. \quad (4.23)$$

As a result the normal projection of the stress jump condition reads:

$$\bar{p} + 2\text{Ca} \varepsilon^{-1} (\bar{u}_{\bar{x}} + h_{\bar{x}} \bar{u}_{\bar{y}}) = -\bar{h}_{\bar{x}\bar{x}} \quad \text{at } \bar{y} = \bar{h}. \quad (4.24)$$

Pressure and capillarity being the dominant terms of order 1 in this expression, there remains two possibilities for the viscous terms: either $\text{Ca}/\varepsilon \ll 1$, either $\text{Ca}/\varepsilon = 1$. In the latter case, this would set the horizontal velocity scale U (thereby using a argument differing from our quick physical picture). With the current state of our asymptotic analysis, we have not enough elements to choose one scenario or the other²⁵.

▷ **Tangential stress continuity.** In absence of space-varying surface tension, the tangential stress continuity reads:

$$\mathbf{n} \cdot (\boldsymbol{\sigma}_{\text{ext}} - \boldsymbol{\sigma}_{\text{int}}) \cdot \mathbf{t} = 0 \quad \text{at the interface } y = h. \quad (4.25)$$

This equation can be explicited as:

$$(p - P_{\text{atm}}) h_x - 2\mu u_x h_x + \mu (u_y + v_x) (1 - h_x^2) - (p - P_{\text{atm}}) h_x + 2\mu v_y h_x = 0. \quad (4.26)$$

To see more clearly the magnitude hierarchy between the different terms, we nondimensionalise this condition:

$$\mu \frac{U}{H} (-2\varepsilon^2 \bar{u}_{\bar{x}} \bar{h}_{\bar{x}} + (\bar{u}_{\bar{y}} + \varepsilon^2 \bar{v}_{\bar{x}}) (1 - \varepsilon^2 \bar{h}_{\bar{x}}^2) + 2\varepsilon^2 \bar{v}_{\bar{y}} \bar{h}_{\bar{x}}) = 0. \quad (4.27)$$

And finally, the expression for this tangential stress-free condition reads to first order:

$$\bar{u}_{\bar{y}} = 0 \quad \text{at } \bar{y} = \bar{h}. \quad (4.28)$$

4.4.3 Flow motion: analysis of the momentum equation

We continue to develop our asymptotic analysis by following the canvas of our quick physical analysis. We now set out to analyse the momentum equation taken along the **principal direction of motion**, that is, the horizontal direction.

▷ **Horizontal momentum balance equation.** Writing the Navier-Stokes equation along the x -direction we have:

$$\underbrace{\rho \frac{U}{T} \bar{u}_{\bar{t}} + \rho \frac{U^2}{\lambda} \bar{w} \bar{u}_{\bar{x}} + \rho \frac{U^2}{\lambda} \bar{v} \bar{u}_{\bar{y}}}_{\text{consequence}} = - \underbrace{\gamma \frac{H}{\lambda^3} \bar{p}_{\bar{x}}}_{\text{driving force}} + \underbrace{\mu \frac{U}{H^2} (\varepsilon^2 \bar{u}_{\bar{x}\bar{x}} + \bar{u}_{\bar{y}\bar{y}})}_{\text{viscous braking}}. \quad (4.29)$$

In this equation we have introduced the new variable \bar{t} defined as $t = T\bar{t}$. T is a natural timescale of the problem, which could be for example the period of an external forcing. Without such a forcing, we can take the inertial timescale²⁶ $T = \lambda/U$, so that the entire left hand side scales as $\rho U^2/\lambda$.

Guided by our initial picture, we here want to take pressure (the driving force) and viscosity (braking) as the dominant factors. This leads us to **set** the velocity scale U so that:

$$\text{Ca} = \varepsilon^3, \quad (4.30)$$

²⁵although we do know, from our previous analysis, that eventually we will find $Ca \sim \varepsilon^3$!

²⁶We could have chosen a different timescale. For example, if we use the diffusive timescale $T_{\text{diff}} = \rho H^2/\mu$, we would retain $\bar{u}_{\bar{t}}$ in the final asymptotic form, but then our analysis would be focused on very short times $O(T_{\text{diff}})$ where momentum diffuses across the film. This timescale being very short in front of the convective timescale $T_{\text{conv}} = \lambda/U$, the film can be seen as “frozen” with this choice: indeed the ratio between these timescales $T_{\text{diff}}/T_{\text{conv}} = \varepsilon \text{Re}$ will be found to be of order $\sim 10^{-8}$ at the end of the study.

which can be rewritten as:

$$U = \frac{\gamma}{\mu} \left(\frac{H}{\lambda} \right)^3. \quad (4.31)$$

We can then rewrite (4.29) under the following nondimensional form:

$$\underbrace{\frac{\rho\gamma H^5}{\mu^2 \lambda^4}}_{\equiv \varepsilon \text{Re}} (\bar{u}_{\bar{t}} + \bar{u}\bar{u}_{\bar{x}} + \bar{v}\bar{u}_{\bar{y}}) = -\bar{p}_{\bar{x}} + \bar{u}_{\bar{y}\bar{y}}. \quad (4.32)$$

For our analysis to be consistent, the left hand side should be much less than – or at worse of the same order of – the right hand side (of order 1). Evaluating $\rho\gamma H^5/\mu^2 \lambda^4$ (which can be rewritten as εRe , with $\text{Re} = \rho U H / \mu$) with the parameters of the problem yields a value $O(10^{-4})$. The left hand side being four orders of magnitude less than the right hand side, we conclude that to first order the x -momentum equation simply reads:

$$\bar{u}_{\bar{y}\bar{y}} = \bar{p}_{\bar{x}}. \quad (4.33)$$

A second consequence of the scaling law for the velocity (4.30) is that the normal viscous stress of magnitude Ca/ε in the normal stress jump equation (4.24) is indeed negligible in front of the other terms. The final form of the leading order normal stress jump condition is therefore:

$$\bar{p} = -\bar{h}_{\bar{x}\bar{x}} \quad \text{at} \quad \bar{y} = \bar{h}. \quad (4.34)$$

▷ **Vertical momentum balance.** We can perform the same analysis on the vertical component of the momentum equation. The difference now is that every characteristic scale has been set, so there is no degree of freedom left. Conducting the same reasoning as before and nondimensionalising we get:

$$\underbrace{\varepsilon^3 \text{Re} (\bar{v}_{\bar{t}} + \bar{u}\bar{v}_{\bar{x}} + \bar{v}\bar{v}_{\bar{y}})}_{\text{Bo}/\varepsilon^2} = -\bar{p}_{\bar{y}} + \underbrace{\varepsilon^2 (\varepsilon^2 \bar{v}_{\bar{x}\bar{x}} + \bar{v}_{\bar{y}\bar{y}})}_{\text{Bo}/\varepsilon^2} - \frac{\rho g \lambda^2}{\gamma}. \quad (4.35)$$

We see that once again the equation simplifies drastically into the hydrostatics equation. The last nondimensional gravity term evaluates to $\frac{1}{20}$ for the configuration we are interested in, so it could safely be neglected. For the sake of completeness we will however keep it in the remaining and note $\overline{\text{Bo}} = \text{Bo}/\varepsilon^2$.

4.4.4 Structure of the flow within the film

We now have all the elements to determine the liquid flow in the film.

▷ **Pressure.** At the interface level, the pressure is set by the normal pressure jump condition (4.34). Solving the hydrostatics equation (4.35) we get the pressure field in the bulk of the fluid:

$$\bar{p} = -\bar{h}_{\bar{x}\bar{x}} + \overline{\text{Bo}} (\bar{h} - \bar{y}). \quad (4.36)$$

Interestingly we see that the isobars are here vertical, and possibly slightly (linearly) distorted by gravity. This “transparency to pressure” feature is a trademark of thin films and boundary layers.

If pressure depends on the depth, this is not the case of the pressure gradient $\bar{p}_{\bar{x}}$:

$$\bar{p}_{\bar{x}} = -\bar{h}_{\bar{x}\bar{x}\bar{x}} + \overline{\text{Bo}} \bar{h}_{\bar{x}}. \quad (4.37)$$

This property will be helpful in designing a generic expression for the velocity field.

▷ **Velocity field.** Knowing that $\bar{p}_{\bar{x}}$ does not depend on \bar{y} , we can integrate the equation of motion (4.33) vertically from the free surface (because the shear stress is known there) to a point \bar{y} :

$$\int_{\bar{h}}^{\bar{y}} \bar{u}_{\bar{y}\bar{y}} d\bar{y} = \bar{u}_{\bar{y}}(\bar{y}) - \underbrace{\bar{u}_{\bar{y}}(\bar{h})}_{\text{with (4.28)}} = \bar{p}_{\bar{x}} (\bar{y} - \bar{h}). \quad (4.38)$$

A second integration from the bottom (because the velocity is known from the no-slip condition) to a point \bar{y} gives the velocity field:

$$\int_0^{\bar{y}} \bar{u}_{\bar{y}} d\bar{y} = \bar{u}(\bar{y}) = \bar{p}_{\bar{x}} \left(\frac{1}{2} \bar{y}^2 - \bar{h} \bar{y} \right). \quad (4.39)$$

The flow is therefore a half-Poiseuille parabolic profile directed along $-\bar{p}_{\bar{x}}$, i.e. from the high pressure regions to the low pressure regions set by capillarity, consistently with our initial picture.

4.4.5 Connecting the free surface deformation with the flow

The connection between the surface deformation rate and the underlying flow is made possible with the help of the kinematic boundary condition. Using $\mathcal{S}(x, y, t) = y - h(x, t)$ it reads:

$$\frac{d\mathcal{S}}{dt} = -\frac{UH}{\lambda} \bar{h}_{\bar{t}} - \frac{UH}{\lambda} \bar{u} \bar{h}_{\bar{x}} + \frac{UH}{\lambda} \bar{v} = 0 \quad \text{at } \bar{y} = \bar{h}. \quad (4.40)$$

All the terms in this equation have equal magnitude: no simplification can be performed. This equation can however be put into a simpler form thanks to Leibniz' rule of integral derivation:

$$\frac{d}{dx} \int_{a(x)}^{b(x)} f(x, y) dy = \int_{a(x)}^{b(x)} \frac{\partial f(x, y)}{\partial x} dy - a'(x)f(x, a(x)) + b'(x)f(x, b(x)). \quad (4.41)$$

In particular we have:

$$\frac{\partial}{\partial \bar{x}} \int_0^{\bar{h}} \bar{u} d\bar{y} = \underbrace{\int_0^{\bar{h}} \frac{\partial \bar{u}}{\partial \bar{x}} d\bar{y}}_{-\bar{v}(\bar{h})} + \bar{h}_{\bar{x}} \bar{u}, \quad (4.42)$$

allowing us to rewrite the kinematic boundary condition (4.40) as:

$$\frac{\partial \bar{h}}{\partial \bar{t}} + \frac{\partial}{\partial \bar{x}} \int_0^{\bar{h}} \bar{u} d\bar{y} = 0. \quad (4.43)$$

This equation actually corresponds to a global mass balance for the liquid film.

4.4.6 Thin film equation

Inserting in the just derived mass conservation equation (4.43) the structure of the velocity field (4.39) we find:

$$\bar{h}_{\bar{t}} - \frac{1}{3} (\bar{p}_{\bar{x}} \bar{h}^3)_{\bar{x}} = 0. \quad (4.44)$$

Using the pressure gradient calculated earlier, we find the final form of the **thin film equation**:

$$\bar{h}_{\bar{t}} + \frac{1}{3} (\bar{h}_{\bar{x}\bar{x}\bar{x}} \bar{h}^3)_{\bar{x}} - \frac{\overline{\text{Bo}}}{3} (\bar{h}_{\bar{x}} \bar{h}^3)_{\bar{x}} = 0, \quad (4.45)$$

or, in dimensioned form:

$$h_t + \frac{\gamma}{3\mu} (h_{xxx} h^3)_x - \frac{\rho g}{3\mu} (h_x h^3)_x = 0. \quad (4.46)$$

Remarkably, this single equation encodes all the physics at play in the liquid film evolution, starting from the first principles (mass and momentum conservation) to all the boundary conditions (dynamic, kinematic). It was first obtained by Landau & Levich (1942) in order to determine the thickness of the liquid film dragged by a solid plate withdrawn from a liquid bath.

4.5 Epilogue: relaxation time for a rippled liquid film

We are now in a position to conclude the question of the relaxation time of a ripple printed over a thin viscous liquid film. Consider a film profile with a slight disturbance $h(x, t) = H(1 + \delta e^{ikx-t/\tau})$, where $\delta \ll 1$ is the amplitude of the disturbance, $k = 2\pi/\lambda$ the perturbation wavenumber, and where an exponential relaxation of time constant τ has been considered. Injecting this ansatz in the film evolution equation (4.46) we get to first order in δ :

$$-\frac{H}{\tau} + \frac{\gamma}{3\mu} k^4 H^4 + \frac{\rho g}{3\mu} k^2 H^4 = 0, \quad (4.47)$$

so that the relaxation time is:

$$\tau = \frac{3\mu}{(\gamma k^4 + \rho g k^2) H^3}. \quad (4.48)$$

In the limit of surface tension dominated evolution considered in the first analysis, the relaxation time reduces to:

$$\tau = \frac{3}{(2\pi)^4} \frac{\mu \lambda^4}{\gamma H^3}. \quad (4.49)$$

Note that we recover our quick order of magnitude estimate (4.12)! This was expected, as we just followed the same steps. But we now have access to the prefactor $3/(2\pi)^4 \simeq 2 \times 10^{-3}$ which is indeed much less than 1. The knowledge of this prefactor allows us to refine our prediction to estimate the relaxation time of our film to be $\simeq 0.25$ s, consistent with the experimental observation.

Chapter 5

Planetary flows and the effect of rotation

Flows at the Earth scale are characterized by considerable horizontal lengthscales (scaling with the radius of the Earth ~ 6000 km) and relatively small vertical lengthscales – atmosphere is typically 10 km-thick and oceans 4 km-deep. The ratio between these lengthscales is $O(1000)$ (which remarkably is similar to the ratio between the radius of a soap bubble and the thickness of the liquid film!). This contrast between lengthscales implies that flows at the Earth-scale will be well captured by thin-film equations.

Another key aspect of planetary flows is **rotation**, which gives rise to particular dynamics, of which cyclones are probably the most impressive illustration. Cyclones owe their existence to the Coriolis force, which imprints its mark on motion over large scales on Earth.

5.1 Rotating fluids

The equations for motion in a rotating frame are best obtained using the Lagrangian formalism. At the fluid particle level, Newton's equation for motion is written:

$$\rho \frac{d^2 \mathbf{r}}{dt^2} = \mathbf{f} \quad (5.1)$$

in an inertial frame. This equation can be rewritten in a rotating frame as:

$$\rho \left(\frac{d^2 \mathbf{r}}{dt^2} + 2\boldsymbol{\Omega} \times \frac{d\mathbf{r}}{dt} + \boldsymbol{\Omega} \times (\boldsymbol{\Omega} \times \mathbf{r}) \right) = \mathbf{f}, \quad (5.2)$$

or:

$$\rho \left(\frac{d\mathbf{u}}{dt} + 2\boldsymbol{\Omega} \times \mathbf{u} + \boldsymbol{\Omega} \times (\boldsymbol{\Omega} \times \mathbf{r}) \right) = \mathbf{f}. \quad (5.3)$$

Expressing the forces, we obtain:

$$\rho \left(\frac{d\mathbf{u}}{dt} + 2\boldsymbol{\Omega} \times \mathbf{u} + \boldsymbol{\Omega} \times (\boldsymbol{\Omega} \times \mathbf{r}) \right) = -\nabla p + \mu \Delta \mathbf{u} + \rho \mathbf{g}_{\text{grav}}. \quad (5.4)$$

The centrifuge force part can be absorbed in a potential called the **geopotential** ϕ :

$$\phi = g_{\text{grav}} z + \frac{1}{2} (\boldsymbol{\Omega} \times \mathbf{r})^2. \quad (5.5)$$

Introducing the effective gravity $\mathbf{g}_{\text{eff}} = -\nabla \phi = \mathbf{g}_{\text{grav}} - \boldsymbol{\Omega} \times (\boldsymbol{\Omega} \times \mathbf{r})$, we can rewrite the equation of motion as:

$$\rho \left(\frac{d\mathbf{u}}{dt} + 2\boldsymbol{\Omega} \times \mathbf{u} \right) = -\nabla p + \mu \Delta \mathbf{u} - \rho \nabla \phi. \quad (5.6)$$

We can non-dimensionalize this equation:

$$\frac{\rho U}{T} \frac{\partial \bar{\mathbf{u}}}{\partial \bar{t}} + \frac{\rho U^2}{L} (\bar{\mathbf{u}} \cdot \bar{\nabla}) \bar{\mathbf{u}} + 2\Omega \rho U \mathbf{e}_z \times \bar{\mathbf{u}} = -\frac{P}{L} \bar{\nabla} \bar{p} + \frac{\mu U}{L^2} \bar{\Delta} \bar{\mathbf{u}} - \frac{\rho \Phi}{L} \bar{\nabla} \bar{\phi}. \quad (5.7)$$

In this expression, we will take for the natural time scale of the problem $T = (2\Omega)^{-1}$ which is the Coriolis pulsation. Further posing $P = \rho U (2\Omega) L$ and $\Phi = 2\Omega U$ to keep the corresponding terms in the equation, we obtain:

$$\frac{\partial \bar{\mathbf{u}}}{\partial \bar{t}} + \text{Ro} (\bar{\mathbf{u}} \cdot \bar{\nabla}) \bar{\mathbf{u}} + \mathbf{e}_z \times \bar{\mathbf{u}} = -\bar{\nabla} \bar{p} + E \bar{\Delta} \bar{\mathbf{u}} - \bar{\nabla} \bar{\phi}. \quad (5.8)$$

Two non-dimensional parameters appear in this equation:

- the **Rossby number** $\text{Ro} = \frac{U}{2\Omega L}$, which quantifies the relative importance of inertial terms with respect to the Coriolis force, and
- the **Ekman number** $E = \frac{\mu}{2\rho\Omega L^2}$, which measures viscous friction relative to Coriolis action.

With a rotation rate of $\Omega = 7.3 \times 10^{-5} \text{s}^{-1}$, we see that atmospheric winds of $\sim 100 \text{ km/h}$ (28 m/s) will be dominated by rotation if $L \gtrsim 200 \text{ km}$. Oceanic flows are much slower; the Gulf Stream, which flows at $U \sim 1 \text{ m/s}$ sees this scale fall down to 7 km . For the same oceanic flows, the Ekman number is $E \sim 10^{-10}$, showing that viscous friction is negligible compared to Coriolis action.

Flows at the planetary scale are therefore strongly influenced by rotation, and to first approximation these flows result from a balance between pressure gradient and Coriolis force. This is the **geostrophic balance**.

5.2 Fluid flows on a rotating sphere

The flows developing on the planet are complex but, depending on their scales, simplifications may be made. Let's investigate these different regimes, starting by writing the equations of motion on a rotating sphere.

5.2.1 Governing equations in spherical coordinates

We have for mass conservation:

$$\frac{d\rho}{dt} + \rho \left(\frac{\partial w}{\partial r} + \frac{2w}{r} + \frac{1}{r \cos \theta} \frac{\partial (v \cos \theta)}{\partial \theta} + \frac{1}{r \cos \theta} \frac{\partial u}{\partial \phi} \right) = 0, \quad (5.9)$$

where (u, v, w) are the velocity components in the (ϕ, θ, r) directions respectively (i.e. longitude, latitude, radius). $\frac{d}{dt}$ stands for the particle derivative operator, which reads in spherical coordinates:

$$\frac{d}{dt} = \frac{\partial}{\partial t} + \frac{u}{r \cos \theta} \frac{\partial}{\partial \phi} + \frac{v}{r} \frac{\partial}{\partial \theta} + w \frac{\partial}{\partial r}. \quad (5.10)$$

The momentum equations take the following form:

$$\left\{ \rho \left(\frac{du}{dt} + \frac{uw}{r} - \frac{uv}{r} \tan \theta - 2\Omega \sin \theta v + 2\Omega \cos \theta w \right) = -\frac{1}{r \cos \theta} \frac{\partial p}{\partial \phi} + \mathcal{F}_\phi, \quad (5.11a) \right.$$

$$\left. \rho \left(\frac{dv}{dt} + \frac{vw}{r} + \frac{u^2}{r} \tan \theta + 2\Omega \sin \theta u \right) = -\frac{1}{r} \frac{\partial p}{\partial \theta} + \mathcal{F}_\theta, \quad (5.11b) \right.$$

$$\left. \rho \left(\frac{dw}{dt} - \frac{u^2 + v^2}{r} - 2\Omega \cos \theta u \right) = -\frac{\partial p}{\partial r} - \rho g + \mathcal{F}_r. \quad (5.11c) \right.$$

Finally the energy equation reads:

$$\rho c_p \frac{dT}{dt} = k\Delta T + Q. \quad (5.12)$$

Here Q represents a possible volumetric heating (e.g. radiative heating from the Sun). Not all the terms in these equations are equally important. In order to identify the leading terms in the previous equations we **choose** relevant scales for the problem and non-dimensionalize the equations.

5.2.2 A local cartesian coordinate system

In order to simplify the previous system of equations, we define the following variables:

$$\begin{cases} x = R\phi \cos \theta_0, \\ y = R(\theta - \theta_0), \end{cases} \quad (5.13a)$$

$$\begin{cases} z = r - R, \end{cases} \quad (5.13b)$$

$$\begin{cases} \end{cases} \quad (5.13c)$$

and relate the derivatives in the two coordinate systems:

$$\begin{cases} \frac{\partial}{\partial \phi} = R \cos \theta_0 \frac{\partial}{\partial x}, \end{cases} \quad (5.14a)$$

$$\begin{cases} \frac{\partial}{\partial \theta} = R \frac{\partial}{\partial y}, \end{cases} \quad (5.14b)$$

$$\begin{cases} \frac{\partial}{\partial r} = \frac{\partial}{\partial z}. \end{cases} \quad (5.14c)$$

5.2.3 Scaling the equations

We now introduce characteristic scales and non-dimensional variables:

$$\begin{cases} x, y = L\bar{x}, L\bar{y}, \end{cases} \quad (5.15a)$$

$$\begin{cases} z = H\bar{z}, \end{cases} \quad (5.15b)$$

$$\begin{cases} u, v = U\bar{u}, U\bar{v}, \end{cases} \quad (5.15c)$$

$$\begin{cases} w = \epsilon\bar{w}, \end{cases} \quad (5.15d)$$

$$\begin{cases} t = \frac{L}{U}\bar{t}, \end{cases} \quad (5.15e)$$

with $\epsilon = H/L \ll 1$ the aspect ratio of the flow.

In order to scale pressure and density, we will consider the atmospheric/oceanic flows to be fluctuations around the hydrostatic equilibrium given by

$$\frac{\partial p_0}{\partial z} = -\rho_0 g, \quad (5.16)$$

i.e. we write:

$$\begin{cases} p = p_0(z) + \tilde{p}, \end{cases} \quad (5.17a)$$

$$\begin{cases} \rho = \rho_0(z) + \tilde{\rho}. \end{cases} \quad (5.17b)$$

If we are located mid-latitude, we expect the pressure to be balanced by the Coriolis acceleration:

$$\rho_0 2\Omega \sin \theta_0 U \sim \frac{\tilde{p}}{L}. \quad (5.18)$$

Noting $f_0 = 2\Omega \sin \theta_0$ the Coriolis parameter at latitude θ_0 , we can therefore scale pressure fluctuations as:

$$\tilde{p} \sim \rho_0 f_0 U L. \quad (5.19)$$

From the vertical momentum equation at leading order, we also have:

$$\frac{\partial \tilde{p}}{\partial z} \sim g \tilde{\rho}, \quad (5.20)$$

which gives the density fluctuation scale:

$$\tilde{\rho} \sim \frac{\rho_0 f_0 U L}{g H}. \quad (5.21)$$

As a result we can write density and pressure as:

$$\begin{cases} p = p_0(z) + \rho_0 f_0 U L \bar{p} = p_0(z) + \frac{\rho_0 U^2}{\text{Ro}} \bar{p}, \end{cases} \quad (5.22a)$$

$$\begin{cases} \rho = \rho_0(z) \left(1 + \frac{f_0 U L}{g H} \bar{\rho} \right) = \rho_0(z) \left(1 + \frac{\text{Ro}}{\text{Bu}} \bar{\rho} \right), \end{cases} \quad (5.22b)$$

Here, Ro is the Rossby number defined previously and $\text{Bu} = L_D^2/L^2$ is the **Burger number**, with $L_D = \sqrt{gH/f_0^2}$ the **Rossby deformation radius**. This characteristic lengthscale delineates flows which are dominated by buoyancy/gravity or geostrophy. Typically, the vortices developing in the Gulf Stream have a size comparable to $L_D \sim 30$ km. For large (quasi-) geostrophic structures, $L \gg L_D$ and $\text{Bu} \ll 1$, but we still obtain a ratio Ro/Bu smaller than unity.

5.2.4 Nondimensionalisation: a worked-out example

Let's rewrite mass conservation with this new set of variables. Noting first that the particle derivative may be written in terms of x , y and z derivatives as:

$$\begin{aligned} \frac{d}{dt} &\equiv \frac{\partial}{\partial t} + \frac{u}{r \cos \theta} \frac{\partial}{\partial \phi} + \frac{v}{r} \frac{\partial}{\partial \theta} + w \frac{\partial}{\partial r} \\ &= \frac{\partial}{\partial t} + u \frac{R \cos \theta_0}{r \cos \theta} \frac{\partial}{\partial x} + v \frac{R}{r} \frac{\partial}{\partial y} + w \frac{\partial}{\partial z}, \end{aligned} \quad (5.23)$$

and that the radius may be connected to the altitude as follows $r = R + H \bar{z} = R + \epsilon L \bar{z} = R(1 + \epsilon \delta \bar{z})$, with $\delta = \frac{L}{R}$, the mass conservation equation can be rewritten as:

$$\begin{aligned} \rho_0 \frac{\text{Ro}}{\text{Bu}} \frac{U}{L} \frac{d\bar{\rho}}{dt} + \rho_0 \left(1 + \frac{\text{Ro}}{\text{Bu}} \bar{\rho} \right) \left(\frac{\epsilon U}{H} \frac{\bar{w}}{\rho_0} \frac{\partial \rho_0}{\partial \bar{z}} + 2 \frac{\epsilon U \bar{w}}{R(1 + \epsilon \delta \bar{z})} \right. \\ \left. + \frac{\epsilon U}{H} \frac{\partial \bar{w}}{\partial \bar{z}} + \frac{R U}{R(1 + \epsilon \delta \bar{z}) L} \frac{\partial \bar{v}}{\partial \bar{y}} - \frac{U}{R(1 + \epsilon \delta \bar{z})} \bar{v} \tan \theta + \frac{R \cos \theta_0}{R(1 + \epsilon \delta \bar{z}) \cos \theta} \frac{U}{L} \frac{\partial \bar{u}}{\partial \bar{x}} \right). \end{aligned} \quad (5.24)$$

This equation can be made dimensionless:

$$\begin{aligned} \frac{\text{Ro}}{\text{Bu}} \frac{d\bar{\rho}}{d\bar{t}} + \left(1 + \frac{\text{Ro}}{\text{Bu}} \bar{\rho} \right) \left(\frac{1}{\rho_0} \frac{\partial \rho_0}{\partial \bar{z}} \bar{w} + 2\epsilon \delta \frac{\bar{w}}{1 + \epsilon \delta \bar{z}} + \frac{\partial \bar{w}}{\partial \bar{z}} + \frac{1}{1 + \epsilon \delta \bar{z}} \frac{\partial \bar{v}}{\partial \bar{y}} \right. \\ \left. - \delta \frac{\bar{v}}{1 + \epsilon \delta \bar{z}} \tan \theta + \frac{\cos \theta_0}{\cos \theta} \frac{1}{1 + \epsilon \delta \bar{z}} \frac{\partial \bar{u}}{\partial \bar{x}} \right) = 0. \end{aligned} \quad (5.25)$$

So far no approximation has been made. But depending on the scale of the flow, several simplifications can be introduced.

▷ **Planetary-sized flows.** For flows at the planet scale, such as the polar vortex flow, we have $\text{Ro}/\text{Bu} \ll 1$, $\epsilon \ll 1$ and $\epsilon\delta \ll 1$. Therefore, at leading order we obtain:

$$\bar{w} \frac{1}{\rho_0} \frac{\partial \rho_0}{\partial \bar{z}} + \frac{\partial \bar{w}}{\partial \bar{z}} + \frac{\partial \bar{v}}{\partial \bar{y}} - \delta \bar{v} \tan \theta + \frac{\cos \theta_0}{\cos \theta} \frac{\partial \bar{u}}{\partial \bar{x}} = 0. \quad (5.26)$$

In this context it is actually more relevant to express the equation back in dimensional form in spherical coordinates:

$$\frac{\rho_0}{r \cos \theta} \left(\frac{\partial u}{\partial \phi} + \frac{\partial (v \cos \theta)}{\partial \theta} \right) + \frac{\partial}{\partial r} (\rho_0 w) = 0. \quad (5.27)$$

▷ **Large-scale atmospheric/oceanic flows.** For large-scale atmospheric or oceanic flows, we still have $\text{Ro}/\text{Bu} \ll 1$ and $\epsilon \ll 1$, but now $\delta \ll 1$ as well. At leading order we obtain the simpler equation in dimensional form:

$$\frac{\partial}{\partial z} (\rho_0 w) + \rho_0 \left(\frac{\partial u}{\partial x} + \frac{\partial v}{\partial y} \right) = 0. \quad (5.28)$$

▷ **Mesoscale flows.** For mesoscale flows, such as oceanic eddies, we have $\delta \ll 1$, $\epsilon\delta \ll 1$, $\text{Bu} \gg 1$, but neither Ro nor ϵ are small a priori. At leading order we now obtain again:

$$\frac{\partial}{\partial z} (\rho_0 w) + \rho_0 \left(\frac{\partial u}{\partial x} + \frac{\partial v}{\partial y} \right) = 0. \quad (5.29)$$

5.2.5 A hierarchy of models for planetary flows

Applying the same scaling analysis to the momentum equations, we obtain a hierarchy of models depending on the scale of the flow considered.

▷ **Planetary-sized flows.** At this scale, the radius of curvature of the Earth cannot be neglected, and the flow appears to be hydrostatic at leading order:

$$\left\{ \begin{array}{l} \frac{\rho_0}{r \cos \theta} \left(\frac{\partial u}{\partial \phi} + \frac{\partial (v \cos \theta)}{\partial \theta} \right) + \frac{\partial}{\partial r} (\rho_0 w) = 0, \\ \rho_0 \left(\frac{du}{dt} - \frac{uv}{r} \tan \theta - 2\Omega \sin \theta v \right) = -\frac{1}{r \cos \theta} \frac{\partial \tilde{p}}{\partial \phi}, \\ \rho_0 \left(\frac{dv}{dt} + \frac{u^2}{r} \tan \theta + 2\Omega \sin \theta u \right) = -\frac{1}{r} \frac{\partial \tilde{p}}{\partial \theta}, \\ \frac{\partial \tilde{p}}{\partial r} = -\tilde{\rho}g. \end{array} \right. \quad (5.30a)$$

$$\left\{ \begin{array}{l} \rho_0 \left(\frac{du}{dt} - 2\Omega \sin \theta_0 v \right) = -\frac{\partial \tilde{p}}{\partial x}, \\ \rho_0 \left(\frac{dv}{dt} + 2\Omega \sin \theta_0 u \right) = -\frac{\partial \tilde{p}}{\partial y}, \\ \frac{\partial \tilde{p}}{\partial z} = -\tilde{\rho}g. \end{array} \right. \quad (5.30b)$$

$$\left\{ \begin{array}{l} \frac{\partial u}{\partial x} + \frac{\partial v}{\partial y} + \frac{1}{\rho_0} \frac{\partial}{\partial z} (\rho_0 w) = 0, \\ \rho_0 \left(\frac{du}{dt} - 2\Omega \sin \theta_0 v \right) = -\frac{\partial \tilde{p}}{\partial x}, \\ \rho_0 \left(\frac{dv}{dt} + 2\Omega \sin \theta_0 u \right) = -\frac{\partial \tilde{p}}{\partial y}, \\ \frac{\partial \tilde{p}}{\partial z} = -\tilde{\rho}g. \end{array} \right. \quad (5.30c)$$

▷ **Large-scale atmospheric/oceanic flows.** At this scale, the curvature of the Earth may be neglected, and the flow appears hydrostatic at leading order:

$$\left\{ \begin{array}{l} \frac{\partial u}{\partial x} + \frac{\partial v}{\partial y} + \frac{1}{\rho_0} \frac{\partial}{\partial z} (\rho_0 w) = 0, \\ \rho_0 \left(\frac{du}{dt} - 2\Omega \sin \theta_0 v \right) = -\frac{\partial \tilde{p}}{\partial x}, \\ \rho_0 \left(\frac{dv}{dt} + 2\Omega \sin \theta_0 u \right) = -\frac{\partial \tilde{p}}{\partial y}, \\ \frac{\partial \tilde{p}}{\partial z} = -\tilde{\rho}g. \end{array} \right. \quad (5.31a)$$

$$\left\{ \begin{array}{l} \frac{\partial u}{\partial x} + \frac{\partial v}{\partial y} + \frac{1}{\rho_0} \frac{\partial}{\partial z} (\rho_0 w) = 0, \\ \rho_0 \left(\frac{du}{dt} - 2\Omega \sin \theta_0 v \right) = -\frac{\partial \tilde{p}}{\partial x}, \\ \rho_0 \left(\frac{dv}{dt} + 2\Omega \sin \theta_0 u \right) = -\frac{\partial \tilde{p}}{\partial y}, \\ \frac{\partial \tilde{p}}{\partial z} = -\tilde{\rho}g. \end{array} \right. \quad (5.31b)$$

$$\left\{ \begin{array}{l} \frac{\partial u}{\partial x} + \frac{\partial v}{\partial y} + \frac{1}{\rho_0} \frac{\partial}{\partial z} (\rho_0 w) = 0, \\ \rho_0 \left(\frac{du}{dt} - 2\Omega \sin \theta_0 v \right) = -\frac{\partial \tilde{p}}{\partial x}, \\ \rho_0 \left(\frac{dv}{dt} + 2\Omega \sin \theta_0 u \right) = -\frac{\partial \tilde{p}}{\partial y}, \\ \frac{\partial \tilde{p}}{\partial z} = -\tilde{\rho}g. \end{array} \right. \quad (5.31c)$$

$$\left\{ \begin{array}{l} \frac{\partial u}{\partial x} + \frac{\partial v}{\partial y} + \frac{1}{\rho_0} \frac{\partial}{\partial z} (\rho_0 w) = 0, \\ \rho_0 \left(\frac{du}{dt} - 2\Omega \sin \theta_0 v \right) = -\frac{\partial \tilde{p}}{\partial x}, \\ \rho_0 \left(\frac{dv}{dt} + 2\Omega \sin \theta_0 u \right) = -\frac{\partial \tilde{p}}{\partial y}, \\ \frac{\partial \tilde{p}}{\partial z} = -\tilde{\rho}g. \end{array} \right. \quad (5.31d)$$

▷ **Mesoscale flows.** At this scale, the curvature of the Earth may be neglected, but the flow is not necessarily hydrostatic at leading order:

$$\begin{cases} \rho_0 \left(\frac{\partial u}{\partial x} + \frac{\partial v}{\partial y} \right) + \frac{\partial}{\partial z} (\rho_0 w) = 0, \end{cases} \quad (5.32a)$$

$$\begin{cases} \rho_0 \frac{du}{dt} = -\frac{\partial \tilde{p}}{\partial x} + fv - f'w, \end{cases} \quad (5.32b)$$

$$\begin{cases} \rho_0 \frac{dv}{dt} = -\frac{\partial \tilde{p}}{\partial y} - fu, \end{cases} \quad (5.32c)$$

$$\begin{cases} \rho_0 \frac{dw}{dt} = -\frac{\partial \tilde{p}}{\partial z} - \tilde{p}g + f'u. \end{cases} \quad (5.32d)$$

5.3 Geostrophic equilibrium

Whenever nonlinear effects and viscous effects are negligible, planetary flows reach an equilibrium known as **geostrophic flow** where:

$$\rho 2\Omega \times \mathbf{u} = -\nabla p. \quad (5.33)$$

Using a local cartesian coordinate system with \mathbf{i} pointing eastwards, \mathbf{j} northwards and \mathbf{k} in the direction of the geopotential gradient, we can write:

$$\mathbf{f} \times \mathbf{u} = -\frac{1}{\rho} \nabla p - \rho \mathbf{g}_{\text{eff}}. \quad (5.34)$$

with $\mathbf{f} = f\mathbf{k}$, $f = 2\Omega \sin \theta$, and θ the latitude. Sometimes f is approximated with a constant value f_0 (f -plane approximation) or linearized around a reference latitude $f = f_0 + \beta y$ (β -plane approximation).

In vertical projection, we recover the hydrostatic balance to first approximation. In horizontal projection, we obtain:

$$\begin{cases} fu = -\frac{1}{\rho} \frac{\partial p}{\partial y}, \end{cases} \quad (5.35a)$$

$$\begin{cases} fv = \frac{1}{\rho} \frac{\partial p}{\partial x}. \end{cases} \quad (5.35b)$$

This implies that $fu \cdot \nabla p = 0$, which means that pressure is constant along streamlines. The pressure plays the role of the streamfunction and the wind follows the isobars! Further, if $f > 0$ (i.e. in the northern hemisphere), the wind is anticlockwise around a low pressure system (cyclonic flows) and clockwise around a high pressure system (anticyclonic flows). This is the **Buyss-Ballot law**.

5.4 Application: wind over France

As an application we will now predict the wind over France using the geostrophic approximation. We suppose that the wind follows the geostrophic equilibrium and that pressure is hydrostatic, i.e.

$$\frac{\partial p}{\partial z} = -\rho \frac{\partial \phi}{\partial z}, \quad (5.36)$$

where ϕ is the geopotential.

It is quite customary to use alternate variables for the vertical scale (it is always possible as long as there is a bijection): pressure, entropy coordinates are therefore routinely used. In pressure

coordinates, we can make use of the following. Let's take a variable ψ depending on (x, y, z, t) and let's rewrite it as a function of (x, y, ξ, t) :

$$\frac{\partial \psi}{\partial \xi} \Big|_{x,y,t} = \frac{\partial \psi}{\partial z} \Big|_{x,y,t} \frac{\partial z}{\partial \xi} \Big|_{x,y,t} ; \quad \frac{\partial \psi}{\partial z} \Big|_{x,y,t} = \frac{\partial \psi}{\partial \xi} \Big|_{x,y,t} \frac{\partial \xi}{\partial z} \Big|_{x,y,t}. \quad (5.37)$$

Similarly for the horizontal derivatives, we get:

$$\frac{\partial \psi}{\partial x} \Big|_{\xi,y,t} = \frac{\partial \psi}{\partial x} \Big|_{z,y,t} + \frac{\partial \psi}{\partial z} \Big|_{x,y,t} \frac{\partial z}{\partial x} \Big|_{\xi,y,t}. \quad (5.38)$$

So, in pressure coordinates:

$$0 = \frac{\partial p}{\partial x} \Big|_{y,z,t} + \frac{\partial p}{\partial z} \Big|_{x,y,t} \frac{\partial z}{\partial x} \Big|_{y,p,t}. \quad (5.39)$$

and

$$\frac{\partial p}{\partial x} \Big|_{y,z,t} = \rho \frac{\partial \phi}{\partial x} \Big|_{y,p,t}. \quad (5.40)$$

and the geostrophic equilibrium reads:

$$\mathbf{f} \times \mathbf{u} = -\frac{1}{\rho} \nabla_p \phi. \quad (5.41)$$

5.5 Oceanic and atmospheric circulation

The fluid envelopes of the Earth are not static: they flow, destabilize into fine turbulence and mix due to complex processes. But at larger scales, the flows in the fluid shells exhibit remarkably stable patterns. Associated with mass, momentum and especially energy transport these flows have a major impact on the climate of the planet. In the following, we examine two remarkable examples of such large-scale flows: the oceanic gyres and the emergence of western boundary currents (such as the Gulf Stream) in the oceans, and the Hadley cell in the atmosphere.

5.5.1 Oceanic circulation: wind-induced gyres

One of the most important factors influencing the climate is the sea surface temperature, which exhibits variations along the latitude of course, but also zonal variations (i.e. along the longitude). To make sense of this temperature distribution, we need to understand the oceanic flows. These are structured in large-scale **gyres** (or vortices). It is noteworthy that these gyres are asymmetric: the **western boundary currents** are much stronger, narrower and deeper than the eastern boundary currents. In the North Atlantic, such an intensification occurs along the US east coast: this is the famous **Gulf Stream**, which transports warm water from the Caribbean up to the North Atlantic, moderating the climate of Western Europe. In the following we will see how these gyres form and why western boundary currents are intensified.

The key role of wind

Somewhat counter-intuitively, the large-scale oceanic circulation is primarily driven by the wind stress at the sea surface. Wind stress is best identified as a source of oceanic motion by considering the African gyre in the Indian Ocean: this gyre reverses seasonally, following the monsoon winds. This suggests that wind is the main driver of the gyres, imparting a shear stress at the sea surface and thereby setting the upper layer of the ocean in motion. In the following, we model this process, following the pioneering work of Henry Stommel (Stommel, 1948).

Stommel's model for wind-driven gyres

We start with the equations expressing geostrophic equilibrium for the ocean:

$$\rho \mathbf{f} \times \mathbf{u} = -\nabla p + \frac{\partial}{\partial z} \boldsymbol{\tau}, \quad (5.42)$$

or in terms of components:

$$\begin{cases} -\rho f v = -\frac{\partial p}{\partial x} + \frac{\partial \tau_{xz}}{\partial z}, \\ \rho f u = -\frac{\partial p}{\partial y} + \frac{\partial \tau_{yz}}{\partial z}. \end{cases} \quad (5.43a)$$

$$\begin{cases} -\rho f v = -\frac{\partial p}{\partial x} + \frac{\partial \tau_{xz}}{\partial z}, \\ \rho f u = -\frac{\partial p}{\partial y} + \frac{\partial \tau_{yz}}{\partial z}. \end{cases} \quad (5.43b)$$

Here, $\boldsymbol{\tau} = (\tau_{xz}, \tau_{yz}, 0)$ stands for the components of the stress tensor associated with vertical transport. We model these stresses using a turbulent viscosity ν_T :

$$\begin{cases} \tau_{xz} = \rho \nu_T \frac{\partial u}{\partial z}, \\ \tau_{yz} = \rho \nu_T \frac{\partial v}{\partial z}. \end{cases} \quad (5.44a)$$

$$\begin{cases} \tau_{xz} = \rho \nu_T \frac{\partial u}{\partial z}, \\ \tau_{yz} = \rho \nu_T \frac{\partial v}{\partial z}. \end{cases} \quad (5.44b)$$

Taking the curl of the geostrophic equilibrium equations (5.43), we obtain:

$$\frac{\partial}{\partial x} (\rho f u) + \frac{\partial}{\partial y} (\rho f v) = \frac{\partial}{\partial z} (\nabla \times \boldsymbol{\tau}). \quad (5.45)$$

Introducing β , the northward gradient of the Coriolis parameter:

$$\beta = \frac{\partial f}{\partial y}, \quad (5.46)$$

we can rewrite the equation (5.45) as:

$$\rho \left(\beta v + f \left(\frac{\partial u}{\partial x} + \frac{\partial v}{\partial y} \right) \right) = \frac{\partial}{\partial z} (\nabla \times \boldsymbol{\tau}). \quad (5.47)$$

Using incompressibility, this equation becomes:

$$\rho \beta v = \rho f \frac{\partial w}{\partial z} + \frac{\partial}{\partial z} (\nabla \times \boldsymbol{\tau}). \quad (5.48)$$

Integrating this equation from the sea floor $z = z_b$ to the sea surface $z = z_t$ we obtain:

$$\rho \beta h \bar{v} = \rho f w|_{z_b}^{z_t} + \nabla \times \boldsymbol{\tau}|_{z_b}^{z_t}, \quad (5.49)$$

This equation calls for a focus on the flow structure near the sea surface and sea floor, where viscous and/or turbulent friction are predominant.

Ekman layers and Ekman pumping

Two completely equivalent choices can now be made: either the equation is integrated exactly to the sea boundaries where the vertical velocity vanishes (at the sea level the vertical velocity is zero on average), either the integration is performed up to the edges of the Ekman layers. Within these layers, the stress vary significantly to match the wind stress at the surface, and the bottom friction on the sea floor, but outside these layers we suppose that the horizontal components of the flow do not vary with height, i.e. that $\boldsymbol{\tau}$ is zero. The vertical velocity is however non-zero in the vicinity of the Ekman layer – a phenomenon known as **Ekman pumping**.

The detailed analysis of the velocity field structure in the Ekman layers reveals that within these regions of typical thickness $\delta = \sqrt{\nu_T/2f}$, the horizontal velocity is observed to spiral and rotate by an angle of $\pi/4$ with respect to the wind direction. This horizontal flow structure does not satisfy $\frac{\partial u}{\partial x} + \frac{\partial v}{\partial y} = 0$ and is therefore associated with a vertical velocity w . Near the sea surface we find:

$$w = \frac{1}{\rho f} \nabla \times \boldsymbol{\tau}_{\text{wind}}. \quad (5.50)$$

At the sea floor, the vertical velocity can be expressed with the bottom friction or alternatively in terms of the geostrophic flow vorticity:

$$w = \frac{\delta}{2} \nabla \times \mathbf{u}. \quad (5.51)$$

Stommel's equation

Including these Ekman pumping effects in the integrated equation (5.49), we obtain:

$$\rho \beta h \bar{v} = \nabla \times \boldsymbol{\tau}_{\text{wind}} - \frac{1}{2} \rho f \delta \nabla \times \bar{\mathbf{u}}. \quad (5.52)$$

Introducing the streamfunction $\psi(x, y)$ such that $\bar{\mathbf{u}} = -\nabla \times (\psi \mathbf{e}_z)$, we have:

$$\bar{u} = -\frac{\partial \psi}{\partial y} \quad ; \quad \bar{v} = \frac{\partial \psi}{\partial x}, \quad (5.53)$$

we start by noting that $\nabla \times \bar{\mathbf{u}} = \Delta \psi \mathbf{e}_z$. We can therefore rewrite the previous equation as:

$$r \Delta \psi + \beta \frac{\partial \psi}{\partial x} = \frac{1}{\rho h} \nabla \times \boldsymbol{\tau}_{\text{wind}}, \quad (5.54)$$

with $r = \frac{1}{2} f \delta / h$ a friction coefficient. This is **Stommel's equation** for wind-driven oceanic gyres. On Earth, if the typical extent of an oceanic basin is $L \sim 5000$ km, then we typically find that $\frac{r}{L} \ll \beta$ indicating that friction is weak compared to the β effect.

A boundary layer?

As friction is small, it is tempting to neglect it altogether. Let's do so and consider a model rectangular ocean basin of typical size L . On the basin boundaries we impose $\psi = 0$. Denoting the typical wind stress scale as τ_0 , we introduce the following non-dimensional variables:

$$\left\{ \begin{array}{l} x, y = L \bar{x}, L \bar{y}, \\ \tau = \tau_0 \bar{\tau}, \end{array} \right. \quad (5.55a)$$

$$\left\{ \begin{array}{l} \psi = \frac{\tau_0}{\rho \beta h} \bar{\psi}. \end{array} \right. \quad (5.55c)$$

$$\left\{ \begin{array}{l} \psi = \frac{\tau_0}{\rho \beta h} \bar{\psi}. \end{array} \right. \quad (5.55c)$$

Noting $\epsilon = r/\beta L \ll 1$, Stommel's equation may be rewritten in non-dimensional form as:

$$\epsilon \Delta \bar{\psi} + \frac{\partial \bar{\psi}}{\partial \bar{x}} = \bar{\nabla} \times \bar{\tau}_{\text{wind}}. \quad (5.56)$$

▷ **Outer solution.** Neglecting friction ($\epsilon = 0$) we obtain the outer solution:

$$\bar{\psi}_0(\bar{x}, \bar{y}) = \int_0^x \bar{\nabla} \times \bar{\tau}_{\text{wind}} d\xi + g(\bar{y}). \quad (5.57)$$

associated with the velocity field:

$$\begin{cases} \bar{u}_0(\bar{x}, \bar{y}) = -\frac{\partial}{\partial \bar{y}} \int_0^{\bar{x}} \bar{\nabla} \times \bar{\tau}_{\text{wind}} d\xi - g'(\bar{y}), \\ \bar{v}_0(\bar{x}, \bar{y}) = \bar{\nabla} \times \bar{\tau}_{\text{wind}}. \end{cases} \quad (5.58a)$$

$$(5.58b)$$

Let's now consider a model wind stress of the form:

$$\bar{\tau}_{\text{wind}} = -\cos(\pi \bar{y}) \mathbf{e}_x, \quad (5.59)$$

which corresponds to a wind blowing eastwards in the northern part of the basin and westwards in the southern part of the basin. The outer solution is therefore:

$$\bar{\psi}_0(\bar{x}, \bar{y}) = \pi \sin(\pi \bar{y}) \bar{x} + g(\bar{y}). \quad (5.60)$$

The boundary conditions at $\bar{y} = 0$ and $\bar{y} = 1$ impose $g(0) = g(1) = 0$. Imposing the western boundary condition corresponds to setting $g(\bar{y}) = 0$. But imposing the eastern boundary condition leads to a contradiction with $g(\bar{y}) = -\pi \sin(\pi \bar{y})$. This means that the outer solution cannot satisfy all boundary conditions: a boundary layer must form either at the western or eastern boundary.

▷ **Boundary layer.** We now introduce a zoomed coordinate near the western or eastern boundary such that $\bar{x} = \delta \tilde{x}$ if the boundary layer is on the west side (in which case $\tilde{x} > 0$), and similarly $\bar{x} - 1 = \delta \tilde{x}$ if the boundary layer is on the east side (in which case $\tilde{x} < 0$). In both cases, Stommel's equation reads:

$$\frac{\epsilon}{\delta^2} \frac{\partial^2 \bar{\psi}}{\partial \tilde{x}^2} + \frac{\partial^2 \bar{\psi}}{\partial \bar{y}^2} + \frac{1}{\delta} \frac{\partial \bar{\psi}}{\partial \tilde{x}} = \bar{\nabla} \times \bar{\tau}_{\text{wind}}. \quad (5.61)$$

The distinguished scaling is obtained for $\delta = \epsilon$, leading to the boundary layer equation:

$$\frac{\partial^2 \bar{\psi}}{\partial \tilde{x}^2} + \frac{\partial \bar{\psi}}{\partial \tilde{x}} = 0. \quad (5.62)$$

The solution for both boundary layers scenarios reads:

$$\tilde{\psi} = A(\bar{y}) e^{-\tilde{x}} + B(\bar{y}) = A(\bar{y}) (e^{-\tilde{x}} - 1). \quad (5.63)$$

While the western boundary layer ($\tilde{x} > 0$) decays exponentially away from the boundary, the eastern boundary layer ($\tilde{x} < 0$) blows up exponentially away from the boundary and is therefore not discarded. As a result, the boundary layer must form on the western boundary, leading to an intensified western boundary current, as observed in the Gulf Stream. Note that the direction of the wind stress is of no importance here, as this forcing term is absent from the boundary layer equations.

▷ **Composite solution.** The composite solution for the streamfunction is therefore:

$$\bar{\psi}(\bar{x}, \bar{y}) = \pi \sin(\pi \bar{y}) (\bar{x} - 1) + A(\bar{y}) (e^{-\bar{x}/\epsilon} - 1) + A(\bar{y}). \quad (5.64)$$

The function $A(\bar{y})$ is determined by imposing the matching condition:

$$A(\bar{y}) = \pi \sin(\pi \bar{y}). \quad (5.65)$$

As a result, the final solution reads:

$$\bar{\psi}(\bar{x}, \bar{y}) = \pi \sin(\pi \bar{y}) (\bar{x} - 1 + e^{-\bar{x}/\epsilon}). \quad (5.66)$$

This solution exhibits a strong western boundary current of typical width $\epsilon L = r/\beta$: the width of the western boundary current is therefore controlled by the friction coefficient r and the β effect.

Bibliography

- ABOURADDY, A. F., BAYINDIR, M., BENOIT, G., HART, S. D., KURIKI, K., ORF, N., SHAPIRA, O., SORIN, F., TEMELKURAN, B. & FINK, Y. 2007 Towards multimaterial multifunctional fibres that see, hear, sense and communicate. *Nat. Mater.* **6** (5), 336–347.
- AITKEN, J. 1873 Glacier motion. *Nature* **7** (172), 287–288.
- ATKINS, PETER 2010 *The laws of thermodynamics: A very short introduction*. Oxford University Press.
- BATCHELOR, G. K. 1967 *An introduction to fluid dynamics*. Cambridge University Press.
- BENNETT, A. 2006 *Lagrangian fluid dynamics*. Cambridge University Press.
- BERRY, M V 1971 The molecular mechanism of surface tension. *Physics Education* **6** (2), 79–84.
- BIRD, R. B., STEWART, W. E. & LIGHTFOOT, E. N. 2002 *Transport phenomena (2nd edition)*. John Wiley & Sons.
- BOYS, C. V. 1890 *Soap bubbles and the forces which mould them*. Thomas Y. Crowell Company.
- CAZABAT, A.-M. & GUENA, G. 2010 Evaporation of macroscopic sessile droplets. *Soft Matter* **6**, 2591–2612.
- CHANDRASEKHAR, S. 1957 *An introduction to the study of stellar structure*. Courier Corporation.
- DE GENNES, P.-G., BROCHARD-WYART, F. & QUÉRÉ, D. 2015 *Gouttes, bulles, perles et ondes*. Belin.
- DUEZ, C., YBERT, C., CLANET, C. & BOCQUET, L. 2007 Making a splash with water repellency. *Nat. Phys.* **3** (3), 180–183.
- DUPRAT, C. & STONE, H. A. 2016 *Fluid-Structure Interactions in Low-Reynolds-Number Flows*. Royal Society of Chemistry.
- EGGERS, J. 2007 Fluid dynamics: Coupling the large and the small. *Nat. Phys.* **3** (3), 145–146.
- ELETTRO, H., NEUKIRCH, S., VOLLRATH, F. & ANTKOWIAK, A. 2016 In-drop capillary spooling of spider capture thread inspires hybrid fibers with mixed solid–liquid mechanical properties. *Proc. Natl Acad. Sci. U.S.A.* **113** (22), 6143–6147.
- ELGETI, J., WINKLER, R. G. & GOMPPER, G. 2015 Physics of microswimmers – single particle motion and collective behavior: a review. *Rep. Prog. Phys.* **78** (5), 056601.
- GHABACHE, ÉLISABETH, ANTKOWIAK, ARNAUD, JOSSERAND, CHRISTOPHE & SÉON, THOMAS 2014 On the physics of fizziness: How bubble bursting controls droplets ejection. *Phys. Fluids* **26** (12), –.

- GOLDSTEIN, S. 1950 *Modern developments in fluid dynamics: an account of theory and experiment relating to boundary layers, turbulent motion and wakes*. Clarendon Press.
- GUAZZELLI, E. & MORRIS, J. F. 2011 *A physical introduction to suspension dynamics*. Cambridge University Press.
- HANCOCK, G. J. 1953 The self-propulsion of microscopic organisms through liquids. *Proc. Roy. Soc. Lond. A* **217** (1128), 96–121.
- HÉNOT, M., GRZELKA, M., ZHANG, J., MARIOT, S., ANTONIUK, I., DROCKENMULLER, E., LÉGER, L. & RESTAGNO, F. 2018 Temperature-controlled slip of polymer melts on ideal substrates. *Phys. Rev. Lett.* **121** (17).
- LANDAU, L. & LEVICH, B. 1942 Dragging of a liquid by a moving plate. *Acta Physicochim. U.R.S.S.* **17**, 42.
- LANGMUIR, IRVING 1918 The evaporation of small spheres. *Phys. Rev.* **12**, 368–370.
- DE LAPLACE, P. S. 1805 *Traité de mécanique céleste. Supplément au livre X*. Courcier, Paris.
- LAUGA, É. 2020 *The fluid dynamics of cell motility*. Cambridge University Press.
- LEAL, L GARY 2007 *Advanced transport phenomena: fluid mechanics and convective transport processes*. Cambridge University Press.
- LIGHTHILL, J. 1986 An informal introduction to theoretical fluid mechanics. *The Institute of Mathematics & its Applications Monograph Series, Oxford: Clarendon Press, 1986*.
- LIGHTHILL, M. J. 1975 *Mathematical Biofluidynamics*. SIAM.
- MAGDELAINE, Q. 2019 Hydrodynamique des films liquides hétérogènes. PhD thesis, Sorbonne Université.
- MARCHAND, A., WEIJS, J. H., SNOEIJER, J. H. & ANDREOTTI, B. 2011 Why is surface tension a force parallel to the interface? *Am. J. Phys.* **79** (10), 999–1008.
- MAXWELL, J. C. 1879 VII. on stresses in rarified gases arising from inequalities of temperature. *Philos. Trans. R. Soc.* **170**, 231–256.
- MAXWELL, J. C. 1890 *Theory of the wet bulb thermometer, in LXXXIX. Diffusion (The scientific papers of James Clerk Maxwell, Cambridge University Press, vol. Vol. 2. Cambridge University Press.*
- MINNAERT, M. 1933 XVI. on musical air-bubbles and the sounds of running water. *Philosophical Magazine* **16** (104), 235–248.
- MITTAL, R., NI, R. & SEO, J.-H. 2020 The flow physics of COVID-19. *J. Fluid Mech.* **894**.
- MOUGIN, G. & MAGNAUDET, J. 2001 Path instability of a rising bubble. *Phys. Rev. Lett.* **88** (1).
- PRANDTL, L. & TIETJENS, O. K. G. 1957 *Applied hydro-and aeromechanics*. Dover publications.
- ROWLINSON, J. S. 2005 *Cohesion: a scientific history of intermolecular forces*. Cambridge University Press.

- SONI, V., BILILIGN, E. S., MAGKIRIADOU, S., SACANNA, S., BARTOLO, D., SHELLY, M. J. & IRVINE, W. T. M. 2019 The odd free surface flows of a colloidal chiral fluid. *Nat. Phys.* **15**, 1188–1194.
- STOMMEL, HENRY 1948 The westward intensification of wind-driven ocean currents. *Transactions American Geophysical Union* **29** (2), 202–206.
- TRYGGVASON, G., SCARDOVELLI, R. & ZALESKI, S. 2011 *Direct numerical simulations of gas–liquid multiphase flows*. Cambridge University Press.
- YOUNG, THOMAS 1805 An essay on the cohesion of fluids. *Philos. Trans. R. Soc.* **95**, 65–87.

Index

- Archimedes principle, 13
- Bond number, 47
- boundary conditions
 - adherence, 27
 - evaporation, 25
 - hydrophobic, hydrophilic, 23
 - imbibition, 24
 - impermeability, 24
 - kinematic, 28
 - no-flux, 25
- Burger number, 58
- Capillary number, 48
- compressibility effects
 - for thin viscous films, 49
- conservation law, 7
 - energy conservation, 17
 - mass conservation, 11
 - momentum conservation, 17
- constitutive laws, 19
- continuity equation, 11
- curvature, 31
- derivative
 - particle, 8, 56
- dissipation, 19
- distinguished scaling, 50
- divergence
 - meaning, 9
 - surface, 34
- drop
 - evaporation, 26
- Ekman pumping, 62
- flux, 7, 10
 - advective, 10
 - diffusive, 11
- geostrophic equilibrium, 60
- Green's function, 43
- Gulf Stream, 61
- gyres, 61
- Laplace pressure jump, 35
- meniscus, 36
- normal vector, 29
- Ohnesorge number, 47
- Rossby deformation radius, 58
- Stokes drag, 42
- Stokes equation, 41
- Stokes reversibility, 42
- Stokeslet, 43
- Stommel's equation, 63
- surface tension, 29
- thin film equation, 53
- turbosail, 24
- velocity (definition), 10
- viscosity, 20
- western boundary currents, 61